Vibration measurements and analyses at ANKA beamline IMAGE in October 2013

Report

by Jörn Groos[1] and Joachim R. R. Ritter[1]

KIT SCIENTIFIC WORKING PAPERS 15

Karlsruhe Institute of Technology

[1] Geophysical Institute

Karlsruhe Institute of Technology

Geophysical Institute
Hertzstr. 16, Bld. 6.42
76187 Karlsruhe, Germany
www.gpi.kit.edu

2013

Abstract

The KIT Geophysical Institute measured the ground motion velocity with six seismometers inside the IMAGE experimental hutch 2 at ANKA. Purpose is the quantitative assessment of the ground motions for the following design of a work-place table with active vibration insulation. The data set of 14 days is analyzed in the time and frequency domains. The ground motions are characterized in two frequency ranges: 1-90 Hz (mainly man-made vibrations) and 0.008-1 Hz (natural vibrations and ground tilt).

Contents

1 Scope of the measurements

Within an internal assignment by ANKA (KIT) and in coordination with the PImicos GmbH, Eschbach, the Geophysical Institute of the KIT conducted vibration measurements in the experimental hutch 2 of the IMAGE beamline at the ANKA synchrotron facility at KIT Campus North (CN). The IMAGE beamline is currently under construction and will be devoted to X-Ray imaging including 3D tomography on a nanometer scale. Purpose of the vibration measurements is the quantitative assessment of the ground motions at the installation site of the experiment for the appropriate design of a work-place table providing sufficient active and passive vibration insulation.

The internal assignment includes:

- Measurement of the ground motion velocity with 3-component-seismometers at three measurement points

- Measurement frequencies: 0.2-50 Hz

- Measurements over seven consecutive days during calendar weeks 43 to 45 in 2013 (ANKA user operation)

- Analysis of the ground motion velocity measurements regarding amplitudes and frequency content and the determination of Peak Ground Velocities (PGV) in appropriate frequency bands

In the following this report provides a brief description of the conducted measurements and a comprehensive analysis of the measured ground motion velocities. Knowledge and experiences from a comprehensive vibration measurement on the KIT CN in 2011 including also one measurement point at ANKA (KIT internal report by Groos & Ritter, 2011) are incorporated into this report. Traffic induced vibrations on the KIT CN are furthermore discussed by Ritter & Sudhaus (2007).

2 Measurement setup

Three mobile seismic stations of the **KA**rlsruher **B**road**B**and **A**rray (KABBA) operated by the Geophysical Institute of the KIT were installed on 16-Oct-2013 and de-installed on 31-Oct-2013. All seismic stations were equipped with 6-channel data acquisition systems, two 3-component broad-band seismometers and near-real time data transmission (see section 2.1). The six seismometers were installed in the **experimental hutch 2** of the ANKA IM-AGE beamline in coordination with responsible ANKA and PImicos personnel (see section 2.2). An on-site inspection to identify local sources of vibrations was done on 24-Oct-2013 15:00-15:50 local time (13:00-13:50 UTC). Only the undisturbed measurements in the time period from 17-Oct-2013 00:00 local time until 30-Oct-2013 23:00 local time (14 days, calendar weeks 42-44) are used for the following analysis.

2.1 Measurement instruments

The used seismometers are modern state-of-the-art 3-component velocity seismometers (force-feedback pendulums) from two different manufacturers and with operational frequency ranges between 8 mHz and 100 Hz. The sensors provide an output voltage proportional to the ground motion velocity. The ground motion velocity is measured in three orthogonal directions in space (one vertical, two horizontal) by every seismometer. The output voltage of each sensor is digitized with a 24 bit A/D converter and stored on hard disk by a data acquisition unit (Earthdata PR6-24). Additionally the data is transferred via internet in near-real time to the KABBA datacenter. The sampling rate is 200 Hz which allows a quantitative analysis of the ground motion velocities up to 90 Hz. All data acquisition units use GPS to achieve a precise time synchronization of the vibration measurements within 10 microseconds.

The conversion of the digital time series in count (integer valued output of the digitizer) to time series of the ground motion velocity (here in mm/s or μm/s) is done with the sensor-specific instrument response functions and gain factors. The description of the seismometer behavior by the nominal linear instrument responses provided by the manufacturers is only valid within the specified operational frequency ranges. Only ground motions within the operational frequency range of the specific sensor can be analyzed in a quantitative way.

The measurements in the experimental hutch 2 of the ANKA IMAGE beamline were conducted with three Streckeisen STS-2 and three Lennartz LE3Dlite seismometers. The data acquisition units were Earthdata PR6-24 seismological data loggers. The relevant properties of the measurement devices are summarized in Table 1.

Seismometer	Gain Sensor in V/(m/s)	Gain A/D-converter in Count/V	Operational frequency range
Streckeisen STS-2	1500	10^6	0.008-45 Hz
Lennartz LE3Dlite	400	10^6	1-100 Hz

Table 1: Relevant properties of the used seismometer types with relevant gain factors and operational frequency ranges.

2.2 Measurement points

The measurement points are located in the experimental hutch 2 of the IMAGE beamline within an area of 2.2 x 4.5 m^2 (Figure 1). The original ANKA hall with the ANKA storage ring was extended in the last years to provide more space for new beamlines. The hall extension is founded on a separate fundament plate. The IMAGE experimental hutch 2 is mainly located in the new part of the ANKA hall but also crosses the fundament plate of the original hall. The planned location of the work-place table is located entirely on the newly build foundation. Five measurement points are located within the planned location of the table and one measurement point is located on the fundament of the original ANKA hall in a distance of about 1 m to the table location.

The measurement points are identified by a station name (CNV06, CNV07 and CNV08) corresponding to the three data acquisition units and a location code (00 and 10) specifying the two sensors connected to each data acquisition unit (Figure 1c, Table 2). The orientation of the horizontal components of the seismometers corresponds to the beam coordinates x (positive in direction of beam propagation) and y (orthogonal to x, positive to the left).

The measurement points CNV06.00 and CNV07.00 are located close to the beam at the southern end of the planned work-place table location. The points CNV06.10 and CNV07.10 are located at the northern end of the planned table location in a distance of 3.2 m in x direction from the points CNV06.00 and CNV07.00. The point CNV08.10 is located at the north-eastern end of the table location.

The measurement point CNV08.00 is located in a distance of about 1 m to the table location on the original ANKA hall foundation which extends about 0.5x0.5 m^2 into the south-eastern corner of IMAGE experimental hutch 2.

Station	Location	Seismometer	Position
CNV06	00	STS-2	work-place table (southern end)
CNV06	10	STS-2	work-place table (northern end)
CNV07	00	LE3Dlite	work-place table (southern end)
CNV07	10	LE3Dlite	work-place table (northern end)
CNV08	00	STS-2	ANKA main fundament plate
CNV08	10	LE3Dlite	work-place table (north-east)

Table 2: Description of the measurement points with used seismometer type.
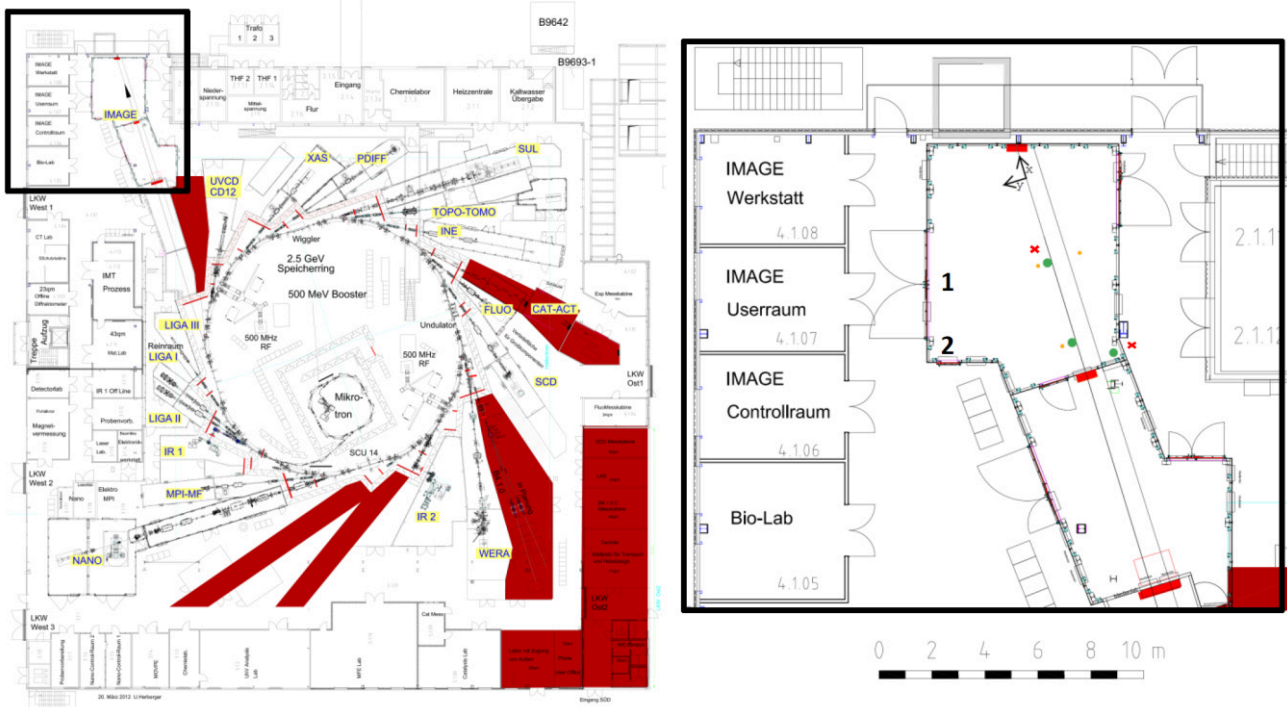
Figure 1: Site plan of the ANKA IMAGE beamline with the measurement points in the IMAGE experimental hutch 2. Top left shows the location of the IMAGE beamline in the ANKA facility.

Top right shows the vicinity of the beamline experimental hutch 2 with corridors and relevant hutch doors (door 1 and 2).

Bottom left shows a close-up of the measurement points together with the station names (CNV0*) and location codes (00/10).

Green circles indicate the positions of the STS-2 seismometers (frequency range 0.008-45 Hz) and orange circles indicate the positions of the LE3Dlite seismometers (frequency range 1-100 Hz). Red crosses mark the standing locations during the ground tilt experiments (see section 6.1).

Measurement point CNV08.00 is located on the corner of the original ANKA hall foundation with extends about 0.5x0.5 m^2 into the IMAGE experimental hutch 2. The remaining measurement points are located on the new foundation built for the extension of the ANKA hall.

3 Data processing and analysis

The digital time series are preprocessed in several steps prior to the quantitative analysis of the ground motion velocities. The first step of preprocessing is the removal of the time series mean (sensor offset) and of a possible linear trend (long term sensor drift). In a second step the time series are convolved with the inverse instrument response to obtain time series of the ground motion velocity. Afterwards the time series are filtered with different bandpass filters to obtain the ground motion velocities in the frequency bands of interest. The bandpass filtering is realized by applying a Butterworth bandpass filter of second order in the time domain. The time series are filtered forward and reverse resulting in an effective fourth order zero-phase bandpass filter. In this way phase distortions of the seismic signals due to the bandpass filtering are avoided.

Next to a direct analysis of the ground motion velocity time series (see Figure 3) also a time-frequency analysis (spectrograms, see Figure 5) is provided. Furthermore, statistical quantities are used to quantify and characterize the ground motions (see Figure 4).

The statistical quantification utilizes the upper boundaries of the 68%, 95.45% and 99.73% amplitude intervals which contain the corresponding amount of measurement values around the time series mean (Figure 2).
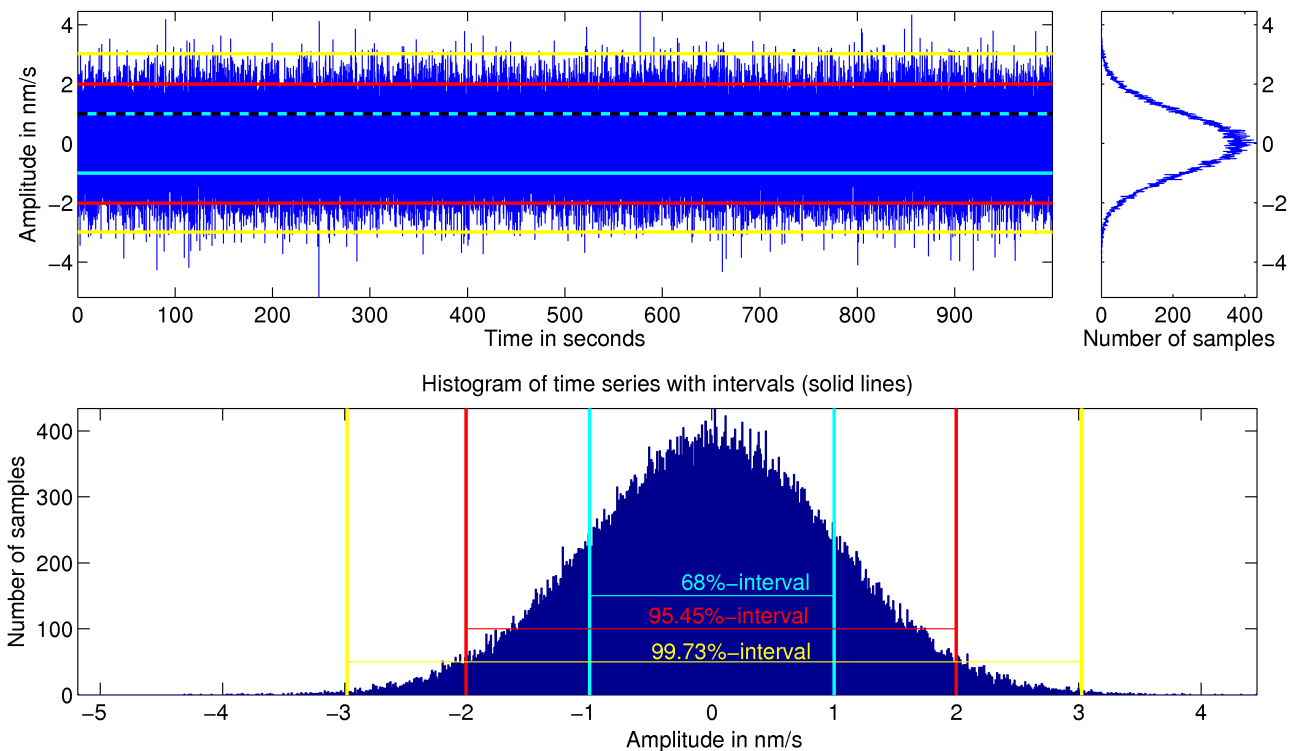
Figure 2: Illustration of the amplitude intervals utilized for the statistical time series quantification by histograms (bottom, top right) of a Gaussian distributed time series (top left) with zero mean and standard deviation 1 nm/s. The upper and lower boundaries of the 68% (cyan), 95.45% (red) and 99.73% (yellow) amplitude intervals, containing the corresponding amount of time series values, are marked with bars and distributed symmetrically around the zero mean.

The utilization of the upper boundary of the intervals is sufficient as the seismic time series have zero mean after preprocessing and exhibit typically a symmetric statistical distribution. The quantification of longer time series (several hours to weeks) is done with a sliding time

window (window and step length is one hour) to reveal temporal variations of the ground motion amplitudes.

A comprehensive description of the spectrogram calculation and the statistical time series quantification is provided in Groos & Ritter (2009).

4 Ambient ground motions / seismic noise

In general, the seismic noise wave field is a superposition of a large amount of (deterministic) seismic signals excited by numerous natural and man-made physical processes. The seismic noise wave field altogether is unpredictable as most individual sources and the structure of the underground are unknown. The seismic noise wavefield is in general dominated by surface waves.

Natural sources of seismic signals in general are tides, water-waves striking the coast, standing water waves in the open seas due to storm systems (ocean-generated microseism), air pressure changes, turbulent wind or wind-induced vibrations of trees or tall buildings. The man-made sources are also numerous such as walking persons, car and train traffic, industrial machines, explosions or the exploitation of underground reservoirs (e.g. hydrocarbons, hot water).

As a rule of thumb, the seismic noise wave field is dominated by signals from natural sources at low frequencies (<0.5 Hz), by man-made sources at high frequencies (>5 Hz) and by both in between (Bonnefoy-Claudet et al., 2006; Groos & Ritter, 2009). An exact separation of both parts of the wavefield by a simple 'border frequency' is not possible and strongly site dependent as it is significantly influenced by the dominant noise sources and the local geological conditions. Man-made sources can dominate the seismic noise wave field down to 0.5 Hz in a setting with a soft subsoil and unconsolidated sediments such as in the Upper Rhine Graben. The dominance of man-made signals ends already above 1 Hz in a hard rook setting. A comprehensive review on seismic noise and its sources is given by Bonnefoy-Claudet et al. (2006) and Groos (2010). A detailed analysis of the ambient ground motions in an urban environment with soft subsoil which is comparable to the setting in the Upper Rhine Graben is presented by Groos & Ritter (2009). A discussion of the seismic noise conditions in the Upper Rhine Graben can be found also in Groos & Ritter (2010).

In the following analysis the corresponding frequency ranges above 1 Hz (section 5) and below 1 Hz (section 6) are discussed separately. The ground motions above 1 Hz are mainly related to the (man-made) sources in vicinity (several meters to a few kilometers) of the IMAGE beamline and subject of the passive and active insulation of the work-place table. The ground motions below 1 Hz caused mainly by far distant (few to thousands of kilometers) sources will be outside the operational frequency band of the active insulation and should be considered as a possible source if undesired effects are observed during experiments at the IMAGE beamline. Below 0.1 Hz also the tilting of the ground due to moving masses (personnel, tram) in vicinity of the experiment should be considered and is therefore discussed in section 6.1.

5 Analysis: ground motions above 1 Hz

The analysis of the ground motions above 1 Hz gives first a general overview about the typical occurring ground motion velocities as well as the Peak Ground Velocities (PGV) observed during the measurement period. Afterwards, the signals caused by the tram (section 5.1), by the doors of the hutch (section 5.2) as well as some electrically driven machinery (section 5.3) are discussed in more detail. It has to be noted here that up to now no machinery (e.g. air conditioning) is installed in the IMAGE experimental hutch 2 and that the hutch was locked for ANKA personnel during the measurements. The observed ground motions represent therefore only signals excited outside the IMAGE experimental hutch 2.

The ground motion velocities (1-90 Hz) at measuring point CNV07.00 during calendar week 43 are shown in Figure 3. The statistical quantification with a sliding time window (window and step length 1 hour) is shown for the vertical ground motion velocities at CNV07.00 and CNV08.10 in Figure 4. It covers the entire measurement period (see Figure 22 and Figure 23 with the horizontal components in the Appendix).
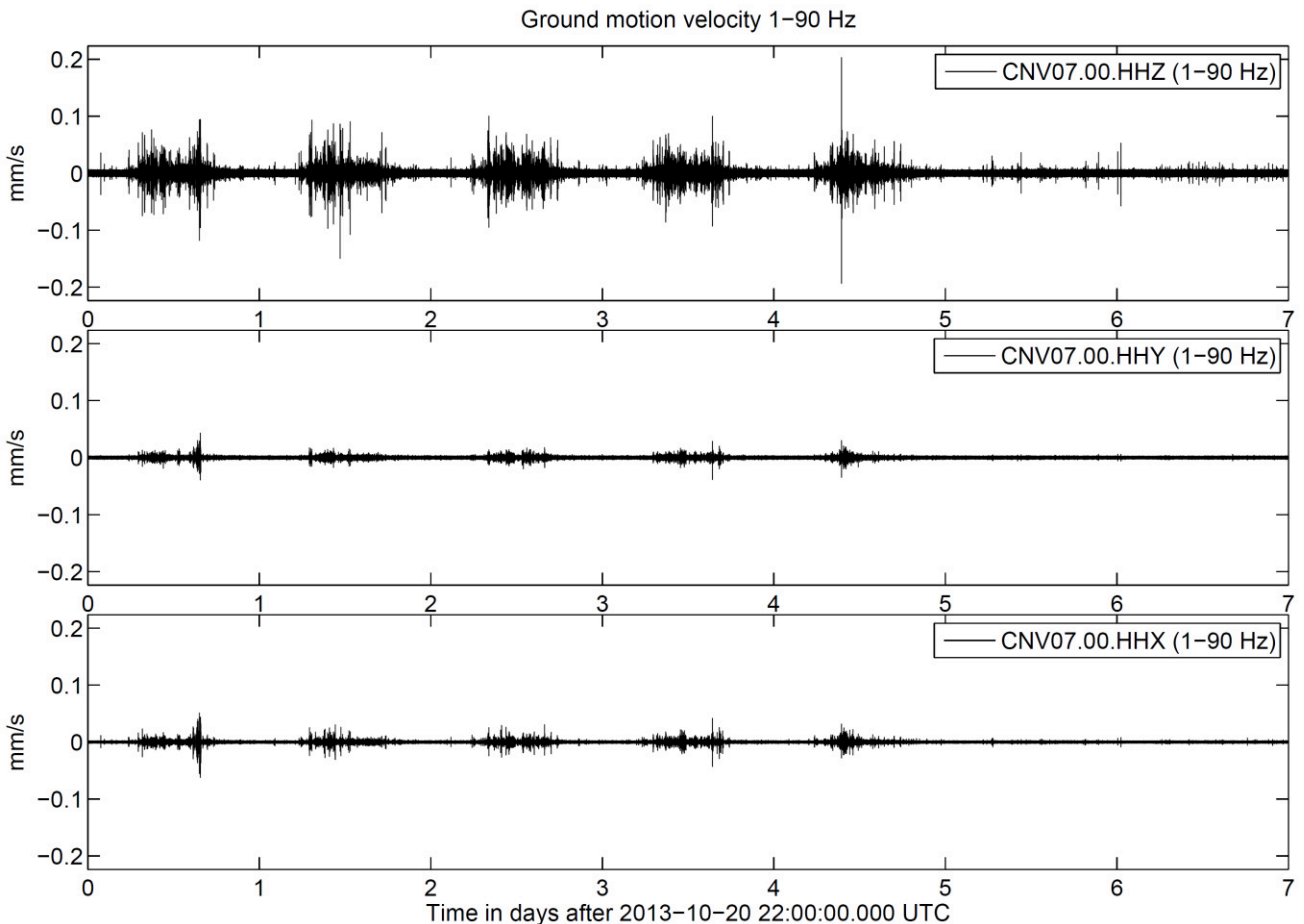
Figure 3: Ground motion velocity on the vertical (Z, top) and the two horizontal (Y, middle and X, bottom) components in the frequency range 1-90 Hz at measuring point CNV07.00 during calendar week 43. The horizontal component coordinates correspond to the beamline coordinates (see Figure 1). The corresponding ground motion acceleration is shown in Figure 21 (Appendix).

The dominant anthropogenic origin of the ground motions above 1 Hz is clearly indicated by the significant variations of the amplitudes with daytime and weekday (Figure 3 and Figure 4). Above 1 Hz the amplitude ratio between the horizontal components and the vertical component (H/V-ratio) is about 0.4 (Figure 3). The largest ground motion amplitudes are

related to transient signals during daytime on working days and are most probably caused by man-made activity in the ANKA building (e.g. construction work, clapping doors) or in direct vicinity to ANKA (e.g. construction work, truck traffic, tram). The transient signals caused by the tram and the hutch doors are discussed in more detail in sections 5.1 and 5.2. The PGV values reach 0.2 mm/s on the vertical component in exceptional cases (Figure 3 and Figure 4). Only for these exceptional transient signals significant (larger than measurement uncertainty) differences between the ground motion amplitudes at the different measurement points within the hutch are observed (Figure 4 bottom). This indicates that these signals were excited by activity in the ANKA hall very close to the IMAGE experimental hutch 2. In general the ground motions at the different measurement points in the hutch show no significant differences (Figure 4). The far most transient signals were smaller than 0.1 mm/s (see 99.73%-interval in Figure 4).
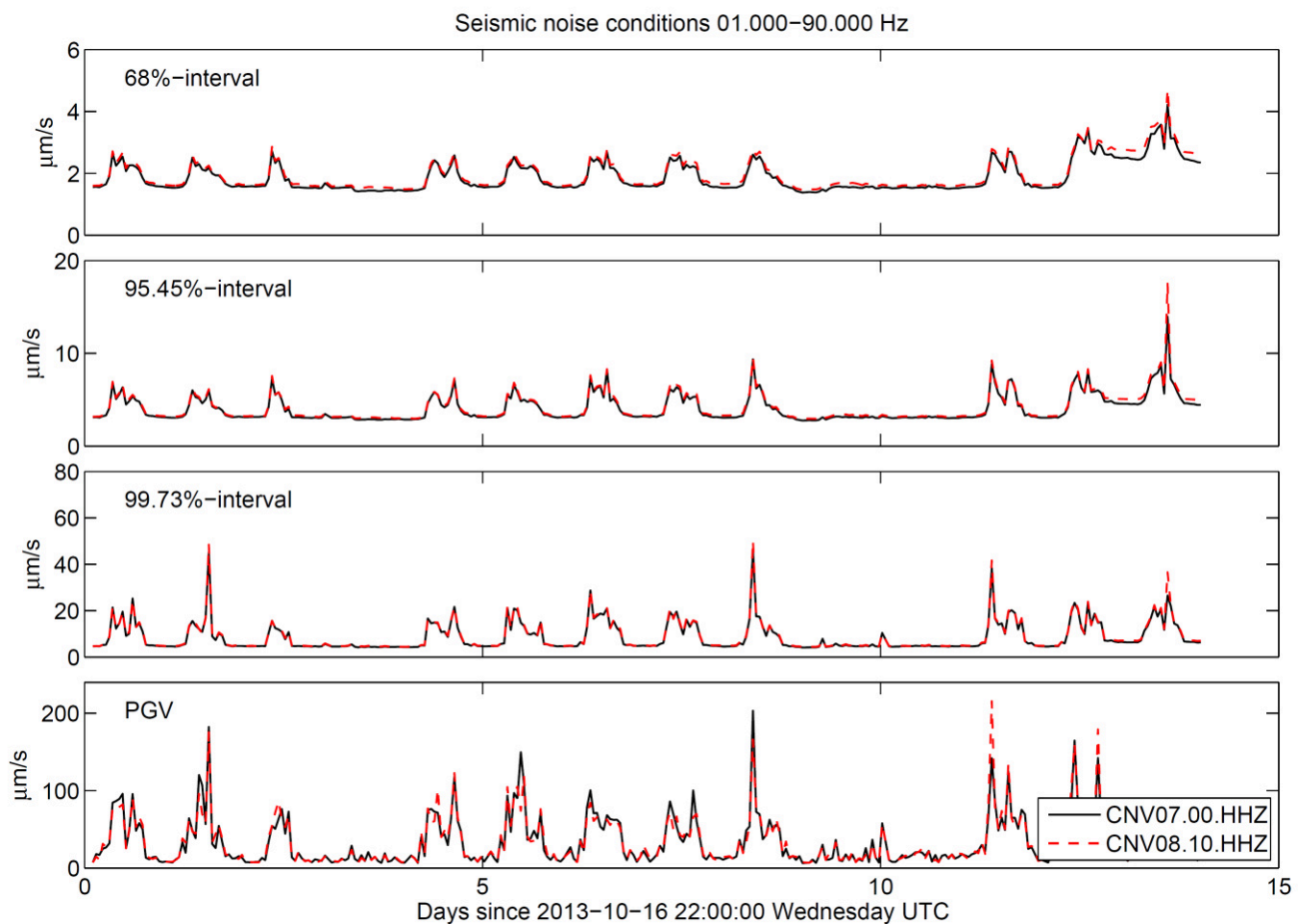
Figure 4: Statistical quantification of the vertical ground motion velocities in the frequency range 1-90 Hz at measurement points CNV07.00 (red) and CNV08.10 (black). Shown are the upper boundaries of the (from top to bottom) 68%, 95.45%, 99.73% and 100% (PGV) amplitude intervals described in Figure 2. The quantities are determined with a sliding time window (window and step length 1 hour) for the time period 17-Oct-2013 to 30-Oct-2013.

It can be concluded from the measurements that PGV values of 0.2 mm/s are the far most vibrations due to typical man-made activity in and around (several hundred meters) ANKA. Nevertheless, it should be considered that significantly higher PGV values up to several mm/s may be reached for example during construction activity inside or close to the ANKA building. The indicative values of DIN 4150-*Vibrations in buildings* suppose ground motions velocities up to 3 mm/s to cause no damages even to sensitive buildings (e.g. historic buildings).

8

The spectrogram in Figure 5 gives a more detailed impression about the ground motions in the IMAGE experimental hutch 2. The transient signals observed on working days during daytime are observed in the frequency range 1-30 Hz with the highest power spectral densities in general. The power spectral densities decrease towards higher frequencies. Horizontal lines reveal periodic (most often sinusoidal) vibrations caused by electrically driven machinery. These signals are the most prominent vibrations above 30 Hz. Most machinery at ANKA is operated 24/7 except the prominent signal at 16.7 Hz and some of the weaker signals between 45 Hz and 50 Hz. These vibrations occur only during beam times of ANKA (see ANKA Status web page). Especially the 16.7 Hz signal (Figure 8) should be considered for the design of the vibration insulation. The periodic vibrations are discussed in more detail in section 5.3.
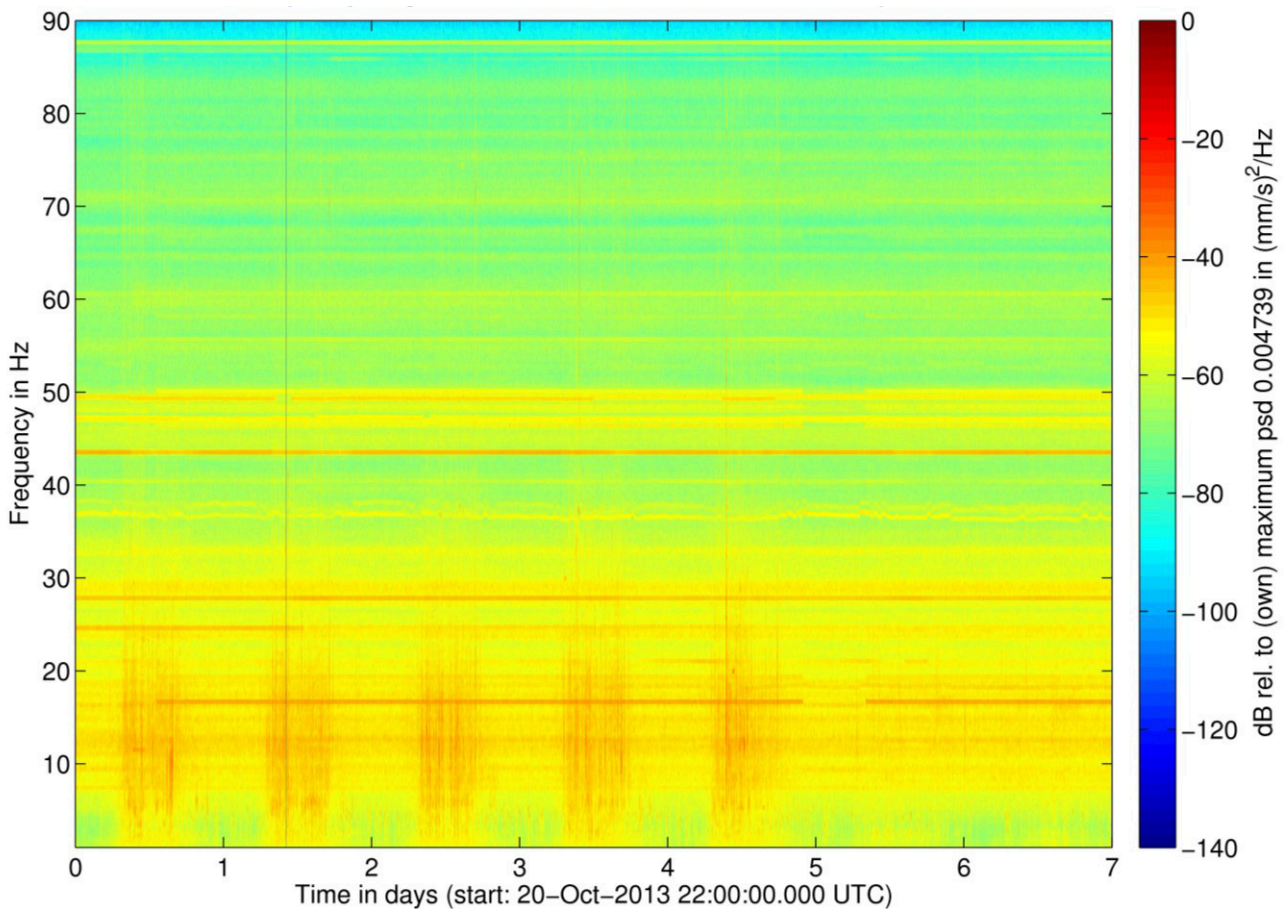
Figure 5: Spectrogram of the vertical ground motion velocity at CNV07.00 in the frequency range 1-90 Hz. The power spectral density (PSD) is shown as a function of time and frequency by a color scale in decibel (dB). Hot colors correspond to high PSDs, cold colors correspond to low PSDs. Above 1 Hz vibrations due to man-made sources dominate the ambient ground motions indicated by systematic variations with daytime and weekday. The highest PSDs are reached by transient signals with frequencies up to 30 Hz which also define the PGV values observed in the time domain (Figure 3). The PSD decreases significantly towards higher frequencies. Horizontal lines of increased PSD indicate periodic vibrations caused by electrical driven machinery (e.g. air conditioning, compressors, …). Such signals are the most prominent vibrations above 30 Hz (see also section 5.3). Most machinery at ANKA is operated in a 24/7 mode. The prominent signal at 16.7 Hz as well as some signals between 45 Hz and 50 Hz are only observable during ANKA beam times (see ANKA status webpage).

5.1 Tram

The tram rails pass ANKA in NWW-SEE direction at about 35 m distance NNE of the IM-AGE experimental hutch 2. The dead-end terminal at KIT Campus North is about 150 m ENE of IMAGE experimental hutch 2. Therefore, the arrival as well as the departure of the trains is observed in terms of transient seismic signals when the trains pass the ANKA hall when entering and leaving KIT Campus North (Figure 6). The excited seismic waves are observed in the frequency range 5-30 Hz with PGV values of about 0.05 mm/s on the vertical component and significantly smaller PGV values on the horizontal components (Figure 6). Next to the propagating seismic waves also a tilt of the ground due to the moving surface load is observed and discussed in more detail in section 6.1.
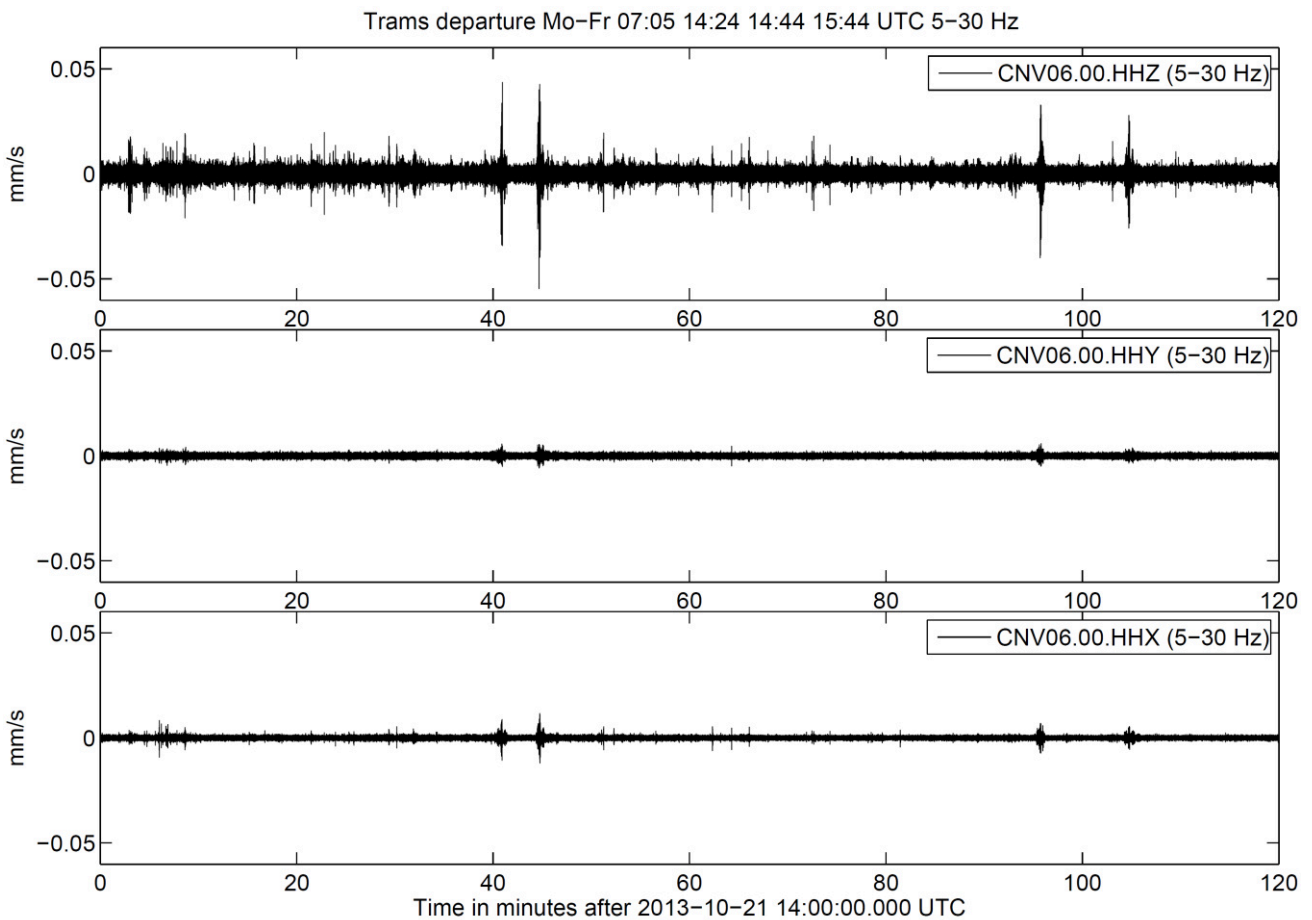
Figure 6: Ground motions in the frequency range 5-30 Hz excited by the passages of the two trams with scheduled departure times 14:44 UTC (minute 44) and 15:44 UTC (minute 104). The arrival as well as the departure of the trains is observed as the KIT Campus North tram station is a dead-end terminal. The analysis of the working days in calendar week 43 reveals that the 15:44 UTC train is typically well on schedule in contrast to the 14:44 UTC train.

5.2 Doors of IMAGE experimental hutch 2

During the on-site inspection on 24-Oct-2013 the two accessible hutch doors (doors marked as 1 and 2 in Figure 1) were opened and closed in an appropriate manner several times. The other doors of experimental hutch 2 were locked or blocked at that time. The excited ground motions observed at CNV07.00 are shown in Figure 7. The closing of the smaller door (door 2) caused signals with PGV values up to 0.03 mm/s (see first three transient signals in Figure 7). The closing of the larger and significantly heavier main door (door 1) caused transient signals with PGV values up to 0.1 mm/s (see the two transient signals after second 80 in Figure 7). Higher PGV values will be reached if the doors are closed faster than necessary or in an uncontrolled manner. It is recommended to close doors of surrounding hutches only carefully during sensitive measurements in the IMAGE experimental hutch 2.
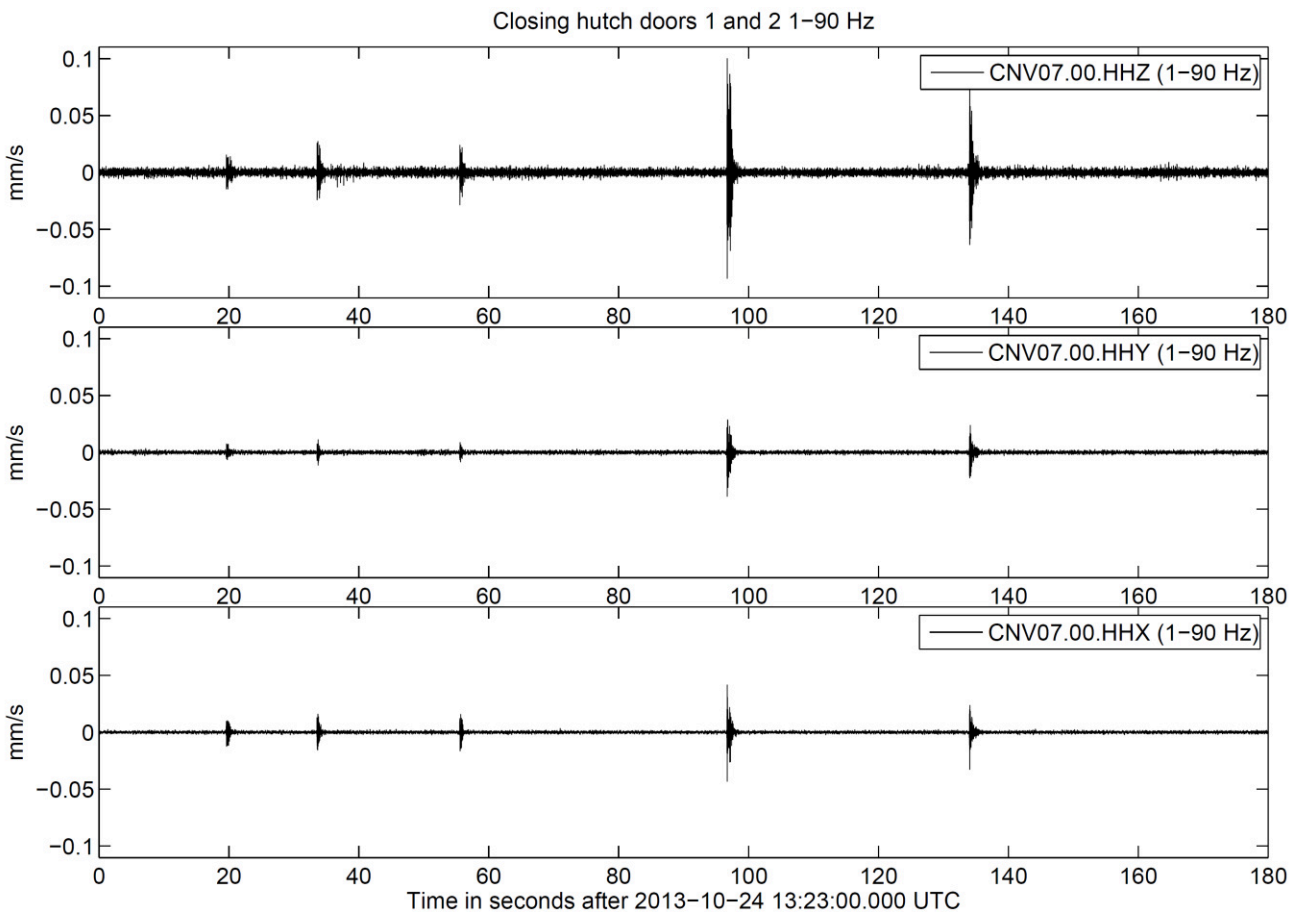
Figure 7: Ground motions in the frequency range 1-90 Hz caused by the appropriate closing of the IMAGE experimental hutch 2 doors 2 (smaller door, first three signals, seconds 18-60) and door 1 (larger main door, two signals, seconds 90-140).The PGV values are observed on the vertical component and reach 0.1 mm/s. Larger PGV values will be reached if the doors are closed in an inappropriate or uncontrolled manner.

5.3 Electrically driven machinery

Vibrations in buildings contain in general periodic, most often sinusoidal, vibrations caused by electrically driven machinery. Most electrical machinery is driven by or contains electrical motors which are operating with engine speeds at or close to integer divisors of the power net frequency (in Germany: 50 Hz). Most common are motors operating close to 50/1 Hz, 50/2 Hz, 50/3 Hz and 50/4 Hz. Nevertheless, frequency changers are commonly used to realize arbitrary engine speeds. All types and sizes of electrical driven machinery are known to cause measurable vibrations in the frequency range above 1 Hz in distances of a few meters (fans, air conditioning) up to several kilometers (e.g. rock crushers). As a rule of thumb it can be assumed, that the frequency of the excited vibrations is increasing with decreasing size of the machinery. The helium compressor of the Institute of Technical Physics (ITEP) at the KIT CN is known to cause significant ground motions with a root mean square (RMS) amplitude of several µm/s at 10 Hz (600 rpm) observable at the entire KIT CN (Groos & Ritter, 2011). The helium compressor is operated only during the experiment periods of ITEP and was not observed during the vibration measurement period in October 2013. Nevertheless, it is advised to consider this known source of significant periodic vibrations at the KIT CN for the design of the vibration insulation system.
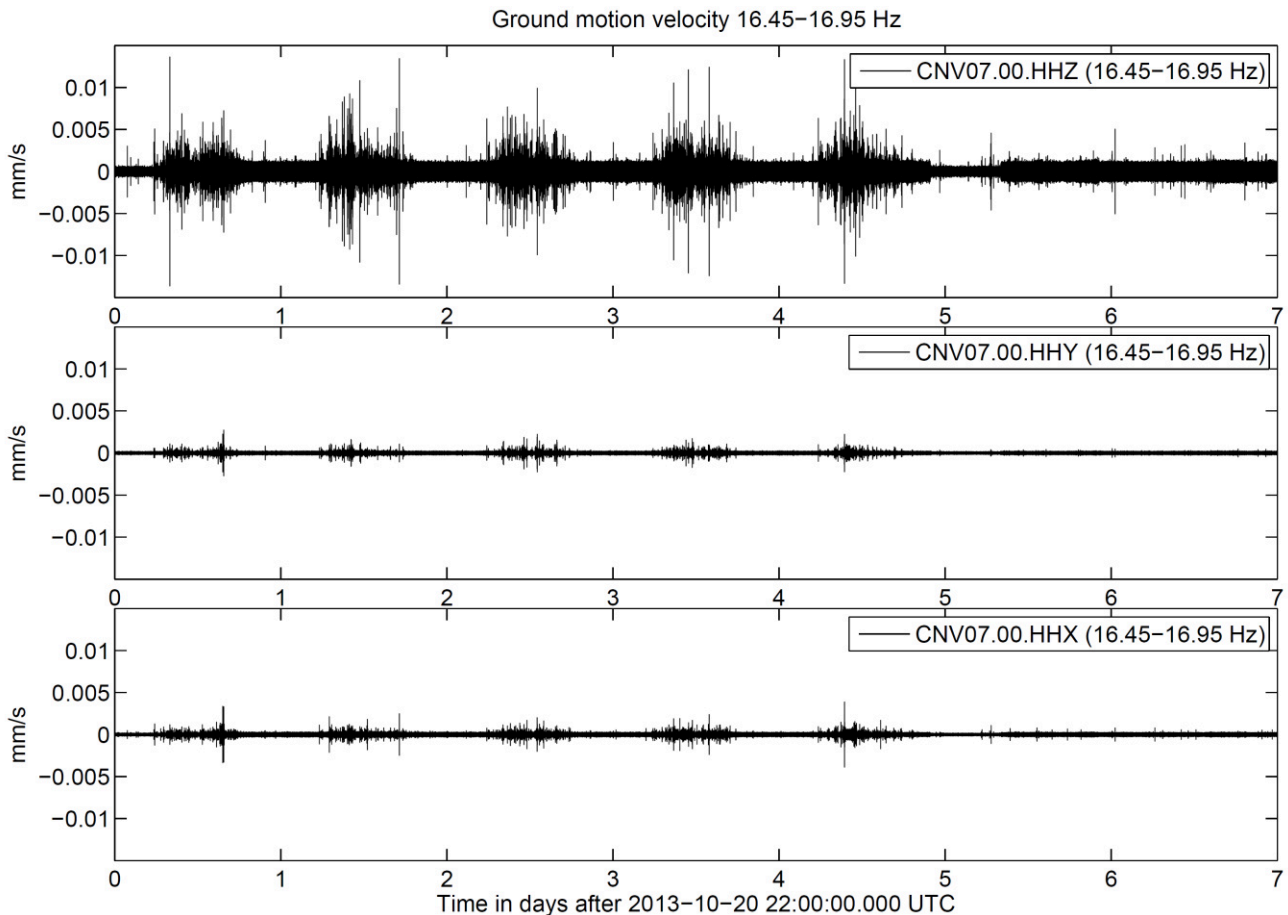
Figure 8: Ground motions in the frequency range 16.45-16.95 Hz (16.7 Hz signal, 0.5 Hz bandwidth) at measurement point CNV07.00. The amplitudes are significantly larger on the vertical component than one the horizontal components and exceed 0.01 mm/s during daytime on working days due to man-made transient signals. The periodic signal itself exhibits PGV values of about 1 µm/s (0.001 mm/s) and RMS amplitudes of about 0.5 µm/s. At the end of day five a sudden offset and on day 6 a sudden onset of the periodic signal can be observed in the time series as well as the spectrogram (Figure 5). These temporal changes coincide with the ANKA beam operation.

The vertical component RMS amplitudes (bandwidth 0.5 Hz) of the most prominent periodic signals observed in the IMAGE experimental hutch 2 at 16.7 Hz, 27.9 Hz, 43.5 Hz, 49.5 Hz and 87.7 Hz (see Figure 5) are shown in Figure 9 for the two measurement points CNV07.00 and CNV08.10. The signals above 16.7 Hz (see also Figure 8) show minor differences in amplitude between the measurement points CNV07.00 and CNV08.10. The RMS amplitude of the signal at 16.7 Hz is affected by the transient signals during daytime at working days but show also two time periods with significantly decreased amplitudes (from about 0.49 μm/s to 0.17 μm/s; see sudden offset on day five in Figure 8). Theses time spans with decreased amplitudes correspond to the times when no beam was provided by ANKA. These vibrations are obviously caused by machinery related to the ANKA operation and will therefore be present during experiments at the IMAGE beamline.
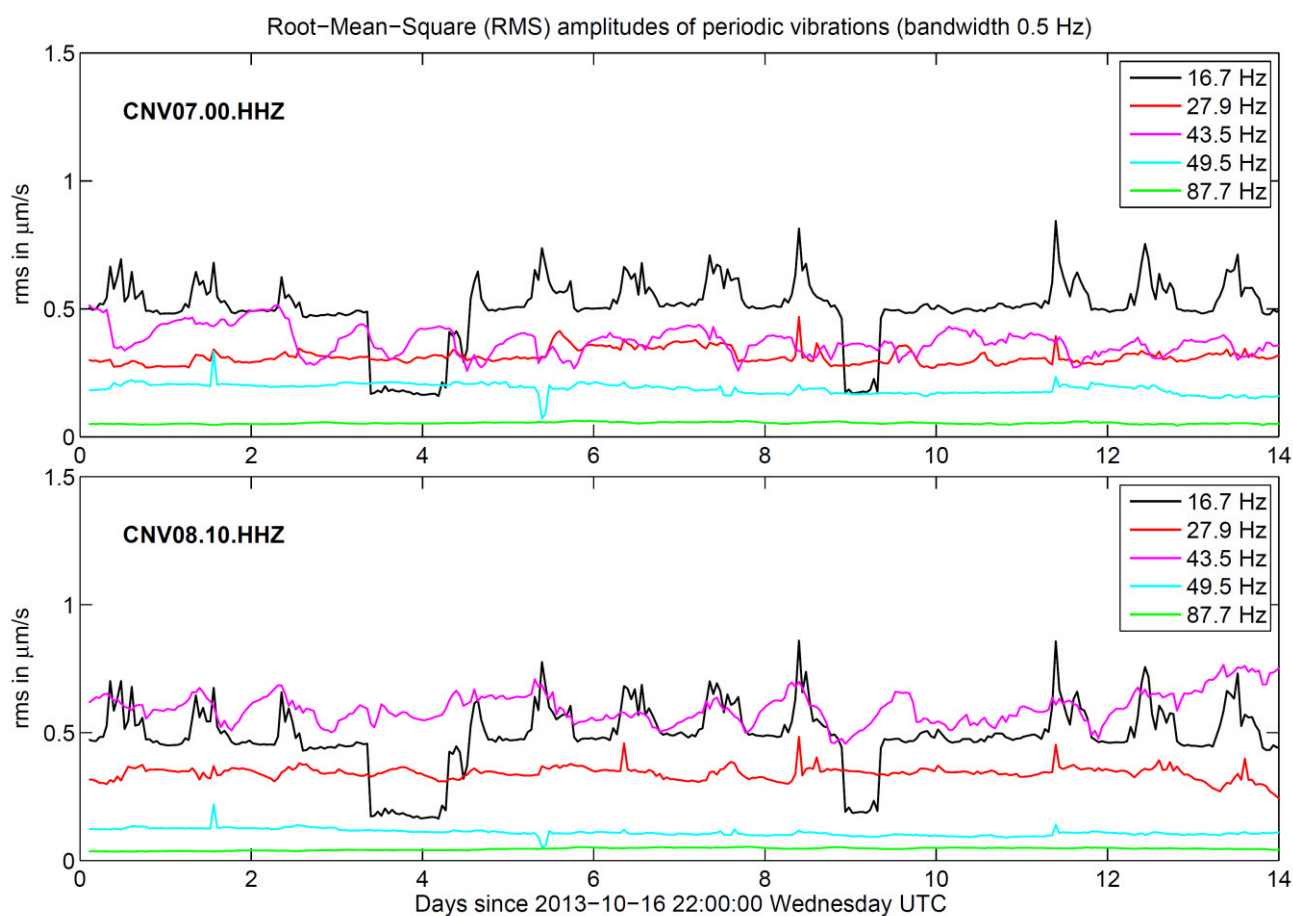
Figure 9: The RMS amplitude of the ground motion velocity in several narrowband (0.5 Hz bandwidth) frequency bands representing the most prominent periodic vibrations observed in the IMAGE experimental hutch 2. The signal at 16.7 Hz shows two time periods with significantly decreased RMS amplitudes during the vibration measurement period. These periods with decreased amplitudes coincide with time periods without beam operation.

6 Analysis: ground motions below 1 Hz

The dominant sources of seismic waves with frequencies below 1 Hz at a given point on earth are earthquakes and ocean-generated microseisms in a distance of a few to several thousand kilometers. Seismic surface waves in the analyzed frequency range 0.008-1 Hz exhibit wavelengths of several hundred meters up to several hundred kilometers. The seismic noise amplitudes due to these signals are nearly identical over the entire KIT CN (Groos & Ritter, 2011) due to their large wavelengths and the local geological conditions.

In Figure 10 the ground motion velocities (0.008-1 Hz) in calendar week 43 are shown for the vertical (Z, top) and the two horizontal (X and Y, see Figure 1) components.
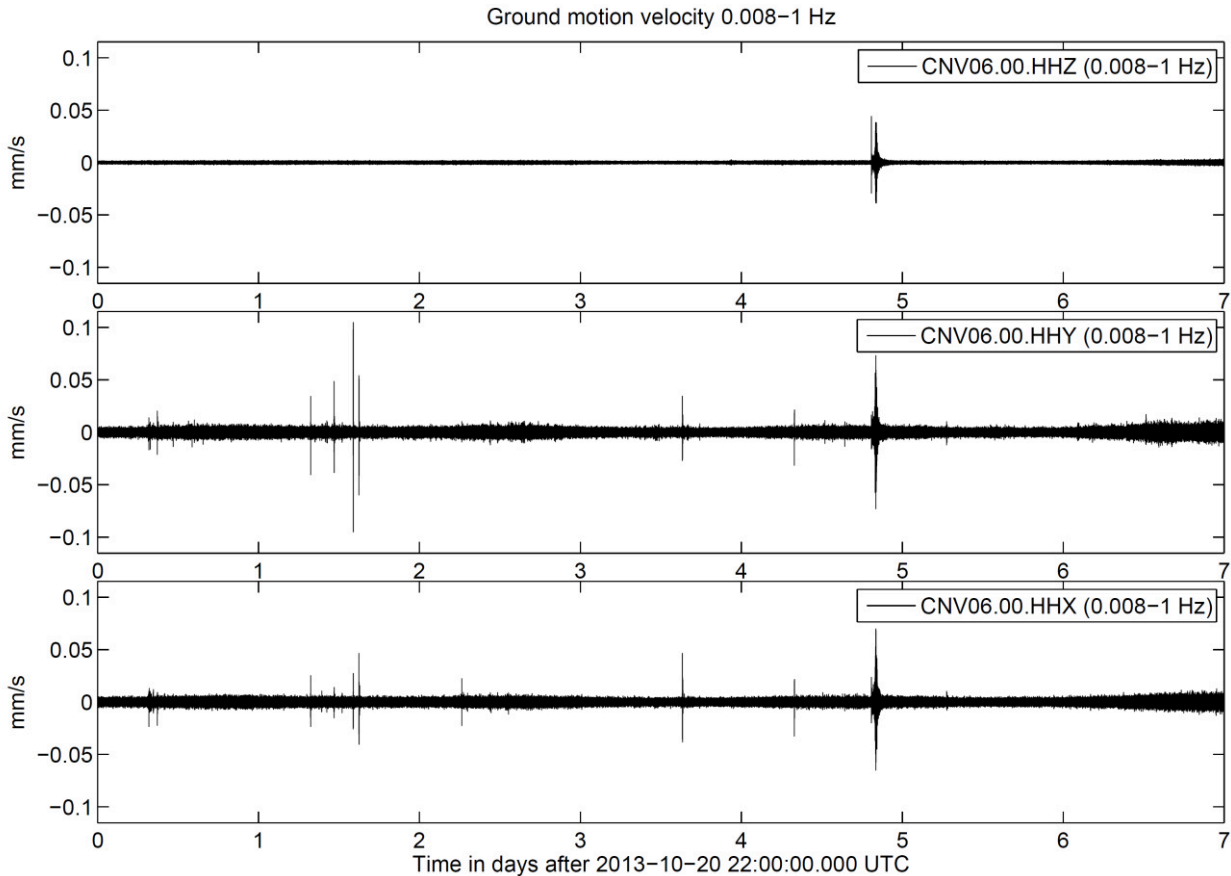
Figure 10: Ground motion velocities on the vertical (Z, top) and the two horizontal (Y, middle and X, bottom) spatial components in the frequency range 0.008-1 Hz at measuring point CNV06.00 during calendar week 43. The horizontal component coordinates correspond to the beamline coordinates.

Below 1 Hz the amplitude ratio between the horizontal components and the vertical component (H/V-ratio) is larger than 1.5 (Figure 10) and it increases towards lower frequencies. The most prominent signal in calendar week 43 with amplitudes larger than 0.05 mm/s on all three components is observed on Friday night. These signals are body and surface waves excited by an earthquake off the East coast of Honshu (magnitude 7.1, distance ~10.000 km, see Figure 11). Depending on magnitude and distance of the earthquakes the PGV values below 1 Hz at ANKA may easily exceed also 0.5 mm/s. The emergent increase of amplitudes on Sunday is due to the increasing ocean-generated microseisms caused by the winter storm *Christian* which started to develop on Saturday over the West Atlantic Ocean and moved then eastwards. *Christian* reached the South-West British coast on Sunday 22:00 UTC and caused severe damage in large parts of Europe in the following days.

14

The transient signals on the horizontal components, occurring typically during daytimes, cannot be interpreted in terms of ground motion velocities as they correspond to the reaction of the force-feedback pendulums to a temporary tilt of the ground caused by the movement of masses in direct vicinity to the sensors. This effect is discussed in detail in section 6.1.

Figure 12 shows the time-frequency analysis (0.008-1 Hz) of the X-component time series (Figure 10, bottom) with high power spectral densities in red colors and low power spectral density in blue colors. The highest power spectral densities are observed due to the surface waves of the Honshu earthquake shown in Figure 11. The increased power spectral densities in the frequency range 0.15-0.4 Hz indicate the perpetual ocean-generated microseism originating from the Atlantic Ocean and the North Sea. The amplitudes and frequency bandwidth of the ocean-generated microseism increase on Sunday due to winter storm *Christian*. Variations of the power spectral density with daytime and weekday are observed at frequencies below 0.1 Hz due to tilt (sources within/very close to the ANKA building) and above 0.6 Hz due to man-made seismic surface waves (sources within a distance of a few kilometers, mainly traffic).
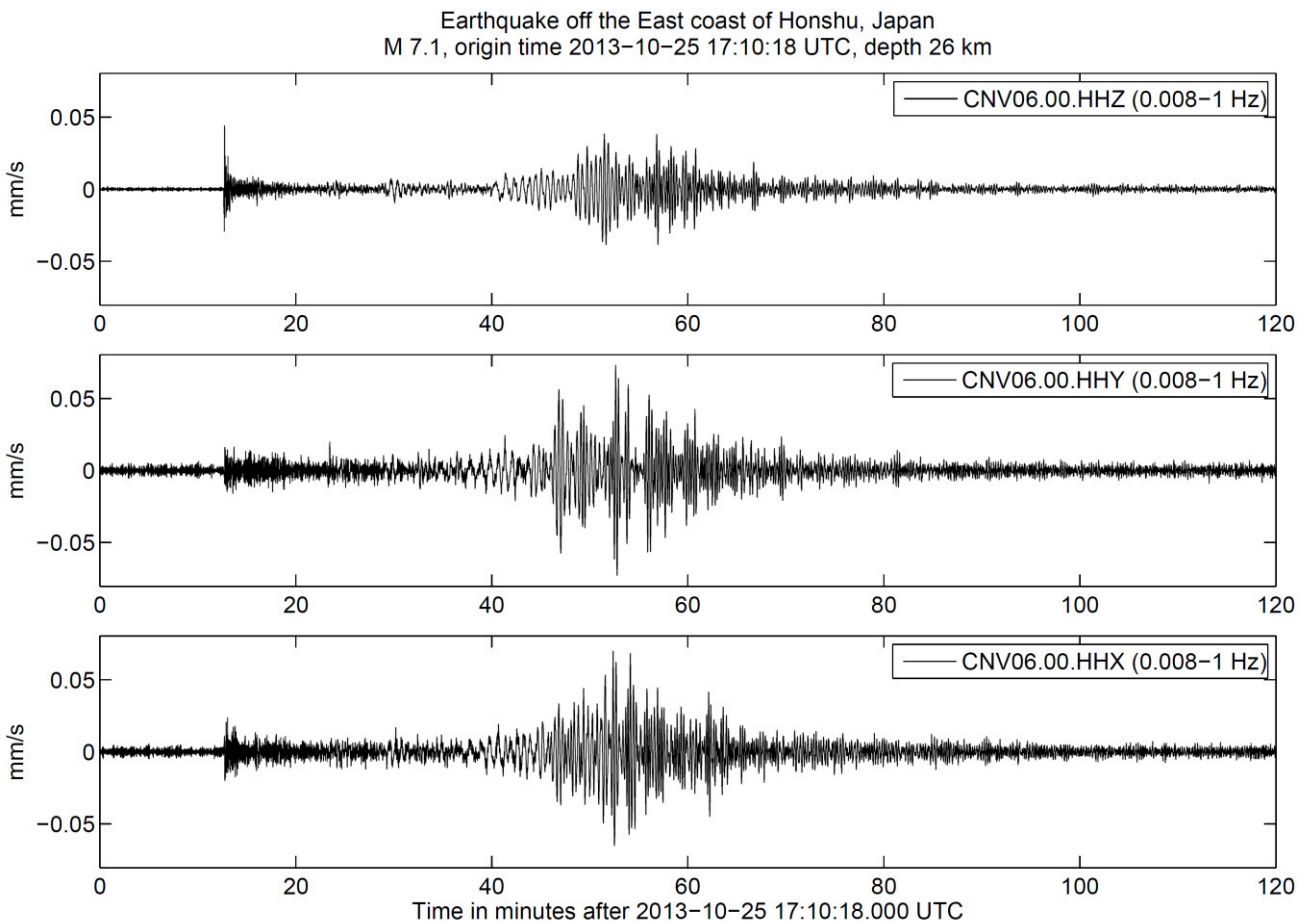
Figure 11: Ground motion velocities due to the magnitude 7.1 earthquake which occurred on 25-Oct-2013 17:10:18 UTC off the East coast of Honshu, Japan. Shown are the vertical (Z, top) and the two horizontal (Y, middle and X, bottom) components of the ground motions in the frequency range 0.008-1 Hz at measuring point CNV06.00. The fastest travelling body waves (pressure waves) arrived at ANKA about 12.5 minutes after the earthquake origin time and reached Peak Ground Velocities (PGV) of about 0.05 mm/s on the vertical component. Even larger PGV values are reached by the later arriving low frequency surface waves on the two horizontal components.

15
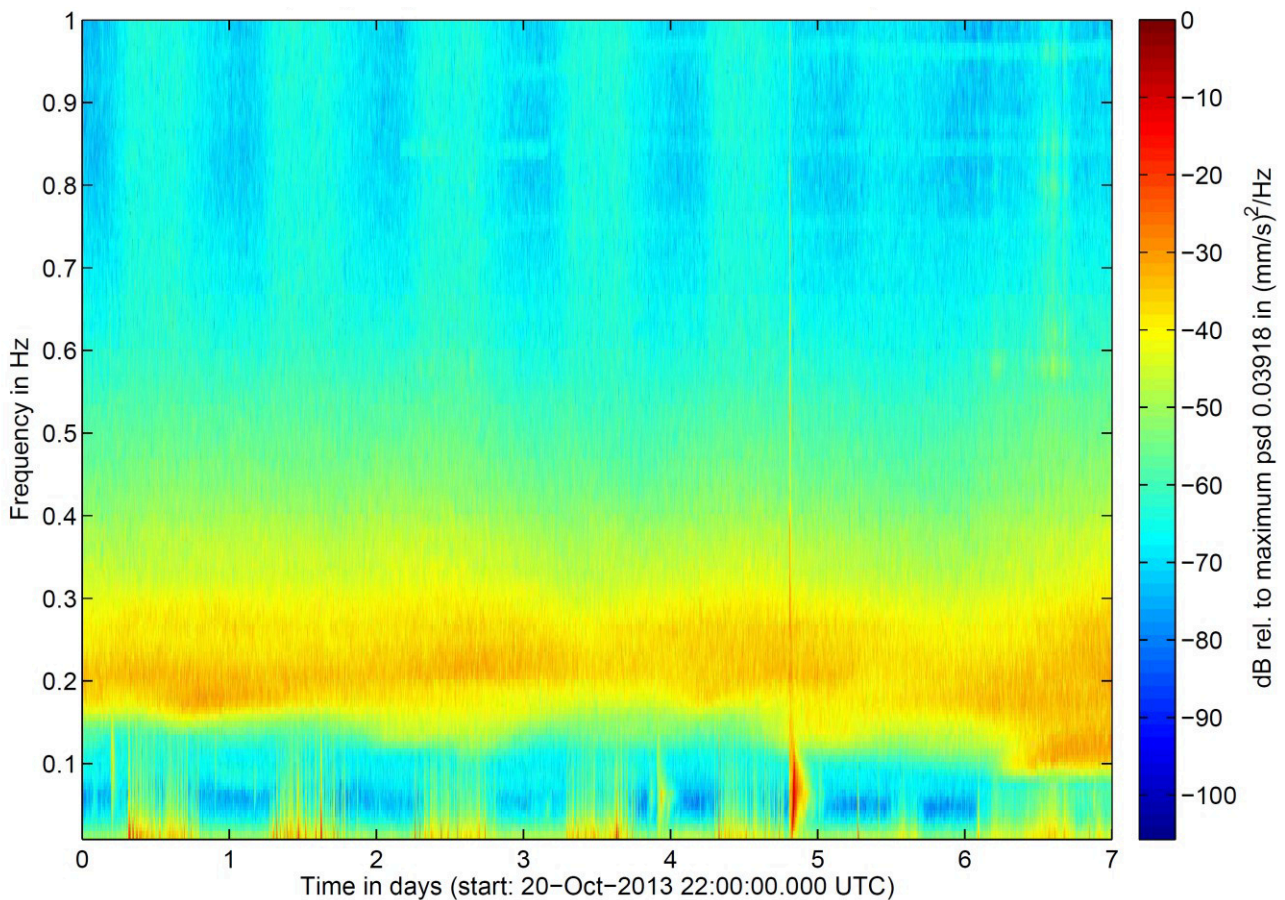
Figure 12: Spectrogram of the horizontal ground motion velocity at CNV06.00 in the frequency range 0.008-1 Hz. The power spectral density is shown as a function of time and frequency by a color scale in decibel (dB). Hot colors correspond to high power spectral densities, cold colors correspond to low power spectral densities. Above 0.6 Hz vibrations due to man-made sources dominate the ambient ground motions indicated by systematic variations with daytime and weekday. In the frequency range between 0.1 Hz and 0.4 Hz surface waves excited by the water waves on the North Atlantic Ocean and the North Sea (ocean-generated microseism) dominate the ground motions at ANKA. The increase of power spectral densities in this frequency range during Sunday is caused by the development of winter storm *Christian* over the West Atlantic Ocean. The highest power spectral densities at all are observed below 0.2 Hz due to the surface waves of the Honshu earthquake shown also in Figure 11. The low frequency signals below 0.1 Hz during daytimes are caused by ground tilt due to moving surface loads (e.g. walking persons, tram) within or in direct vicinity of ANKA (see section 6.1).

6.1 Tilt due to moving masses

Every surface load (mass) causes a tilt (typically in the order of some µrad) of the surrounding ground towards the location of the surface load. The area affected by the tilt depends on the mass and the underground conditions. A standing person typically causes a tilt of the ground of some µrad in a distance up to a few meters.

The output signals of a tilted 3-component force-feedback seismometer (e.g. when a surface load is located close to the sensor) show an apparent accelerated movement of the ground on the horizontal components (Wielandt, 2011; Wielandt & Forbriger, 1999). The gravity acting on the seismic mass of a horizontal seismometer (pendulum) is normally can-

16

celled by its suspension assuming an appropriate leveling of the sensor. If the sensor is tilted due to a tilt of the ground an additional force (projection of gravity in subject to the tilt angle) is acting onto the seismic mass. This is a first-order effect for the horizontal components of a seismometer but only a second-order effect for the vertical component (Wielandt, 2011). From the sensor output the seismometer therefore appears to perform accelerated horizontal movements. If a seismometer experiences a temporary tilt due to a moving mass it will react with a long period transient signal as this transient tilt equals a step like change of ground velocity (Wielandt, 2011). The long period transient signals of the ground motion velocity observed on the horizontal components at frequencies below 0.1 Hz during daytimes on working days (Figure 12) have to be addressed as such signals are caused by a temporary tilt of the ground. Sources are moving masses close to the seismometer locations. To validate these assumptions two experiments were conducted during the on-site inspection on 24-Oct-2013.

Figure 13 shows the apparent ground motion velocities observed by the STS-2 seismometers at points CNV08.00 (red) and CNV06.00 (black).
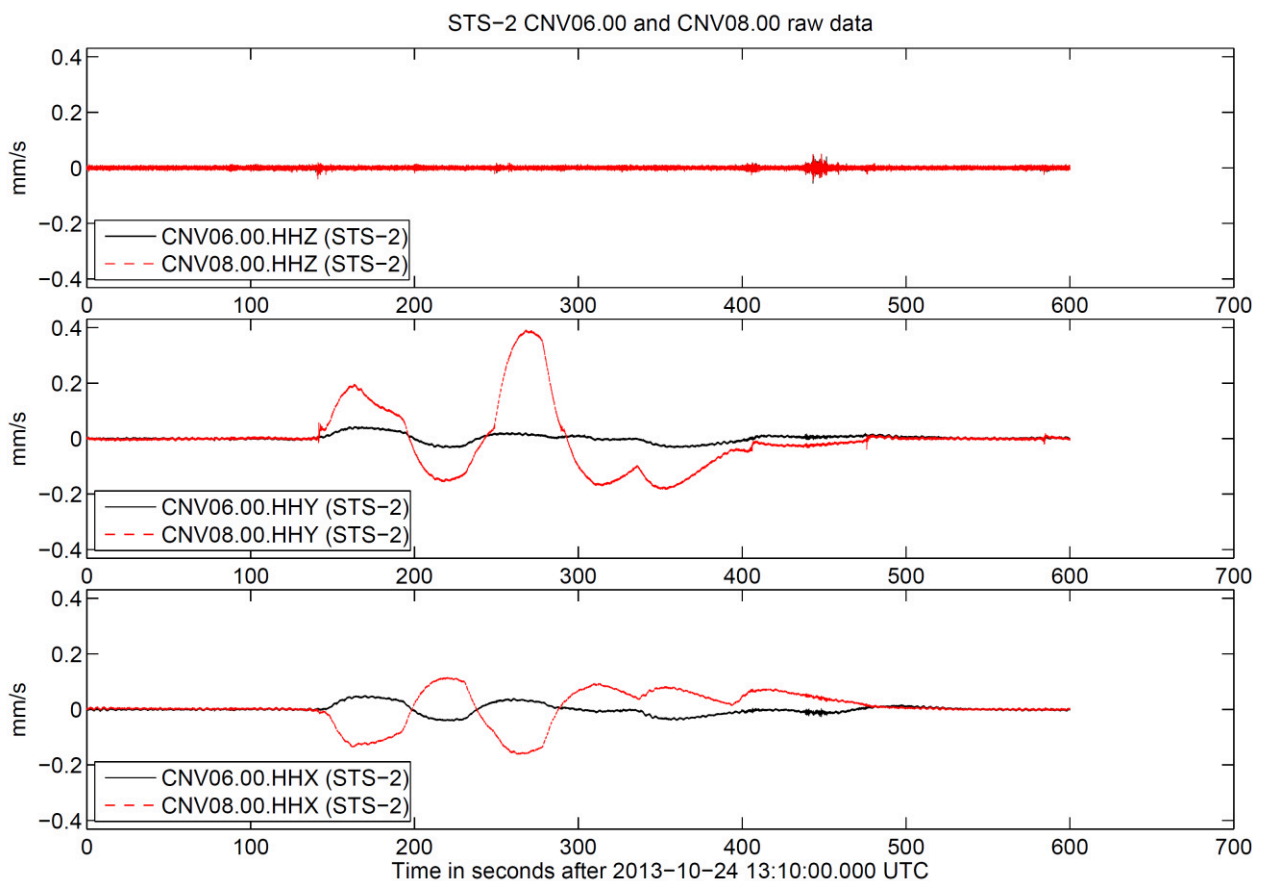
Figure 13: Apparent ground motion velocity observed by the broadband STS-2 seismometers at measurement points CNV06.00 (black) and CNV08.00 (red). The apparent long period accelerated horizontal movements indicate a tilt of the seismometer. The gravity acting on the seismic mass is no longer completely cancelled by the suspension system of the horizontal pendulums if the seismometer is temporary tilted which leads to an apparent accelerated movement of the sensor. The long period signals between second 140 and second 400 are the reaction of the seismometer to the temporary tilt of the ground due to two persons moving and standing next to the sensor outside the hutch in the corridor eastwards of the IMAGE hutch during the on-site inspection (see red cross in Figure 1, top right).

17

During this time two persons approached in the corridor eastwards of IMAGE experimental hutch 2 towards point CNV08.00. They stood outside experimental hutch 2 about 0.5 m next to the seismometer for about one minute (seconds 140 to 200, see red cross outside experimental hutch 2 in Figure 1). Afterwards the persons departed and approached to stand again about one minute next to the sensor (seconds 230 to 290) before they finally departed in the corridor towards the north. The tilt of the seismometers is clearly observed in the sensor output by the apparent long period accelerated horizontal movements. The amplitudes observed at CNV08.00 are significantly larger indicating the significant decrease of the tilt angle with distance to the point load.

The same type of experiment was done at location CNV06.10 within experimental hutch 2. Two persons entered the hutch and stood for about one minute (seconds 420 to 480, see red cross in Figure 1) about 0.5 m next to CNV06.10. The corresponding apparent ground motions are shown for CNV06.00 (black) and CNV06.10 (red) in Figure 14.
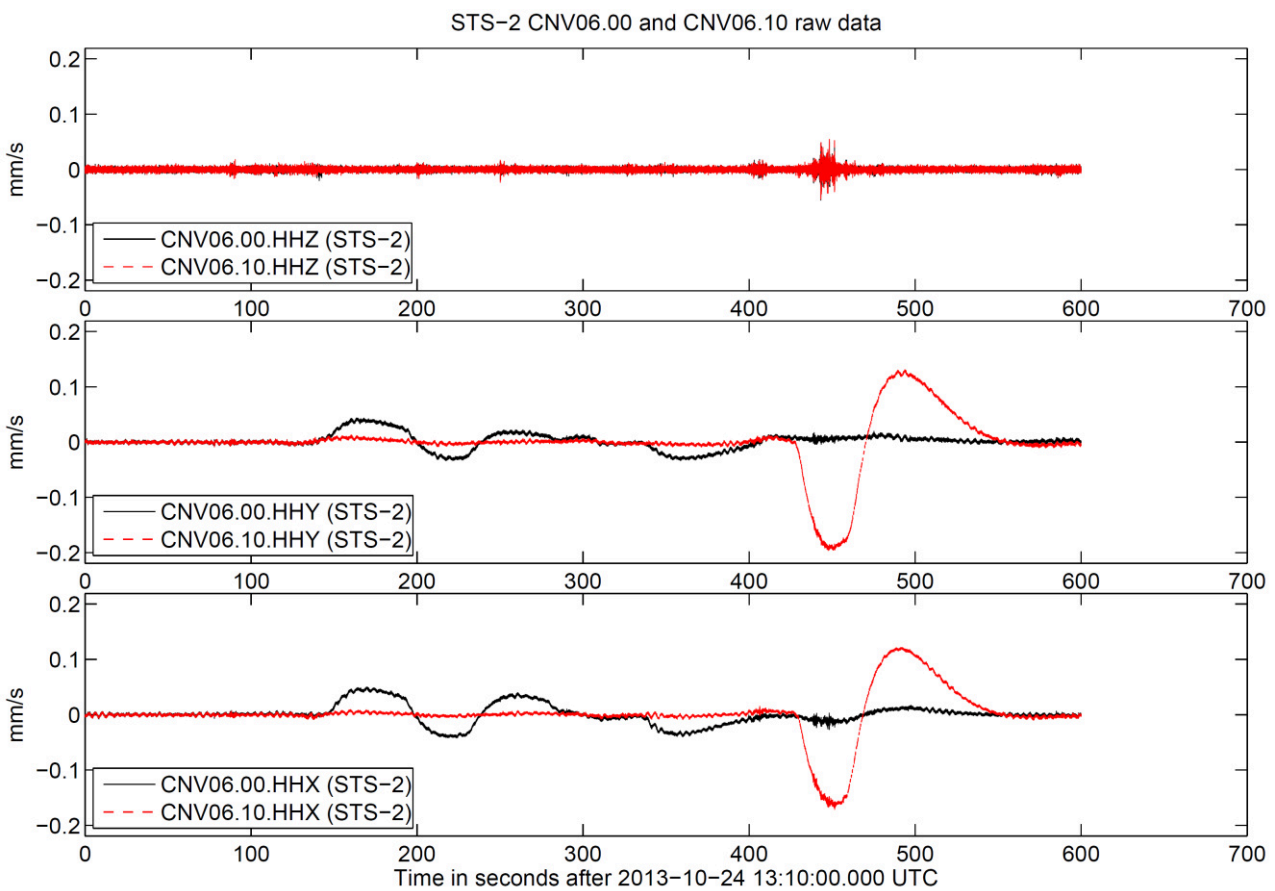
Figure 14: Apparent ground motion velocity observed by the broadband STS-2 seismometers at measurement points CNV06.00 (black) and CNV06.10 (red). The long period signals between second 400 and second 600 are the reaction of the seismometer at CNV06.10 to two persons standing about 0.5 m apart for about one minute (see red cross in Figure 1, top right).

The angle of the seismometer tilt pointing towards the surface load in µrad can be obtained by a careful processing of the raw sensor output data including the removal of the instrument response, a high-pass filtering (here 1800 seconds), a differentiation to acceleration and the multiplication with -1/g. It is furthermore assumed that α ≈ sin α for small tilt angle α. The derived tilt of the seismometers in µrad for the raw data in Figure 13 and Figure 14 is shown in Figure 15 and Figure 16, respectively.
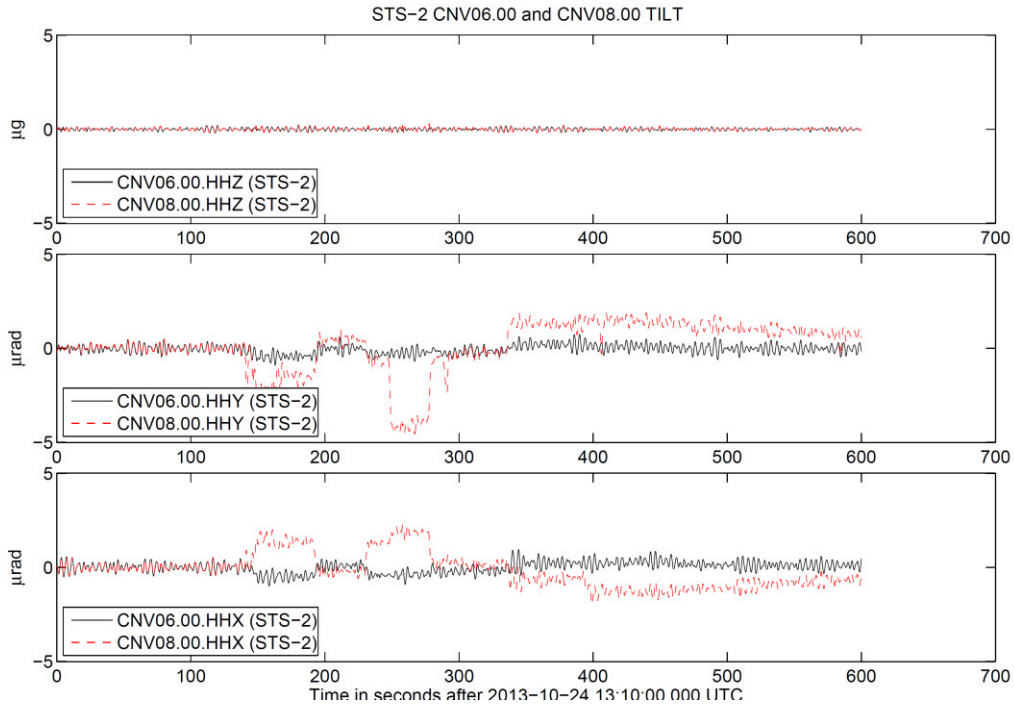
Figure 15: The tilt of the ground at points CNV06.00 (black) and CNV08.00 (red) during the on-site inspection derived by a careful processing of the ground motion velocity time series shown in Figure 13 (details see text). The tilt of the ground during the two periods with two persons standing about 0.5 m next to CNV08.00 (seconds 140-200 and seconds 230-290) reach about 5 µrad. The apparent tilt after second 350 is a processing artefact.
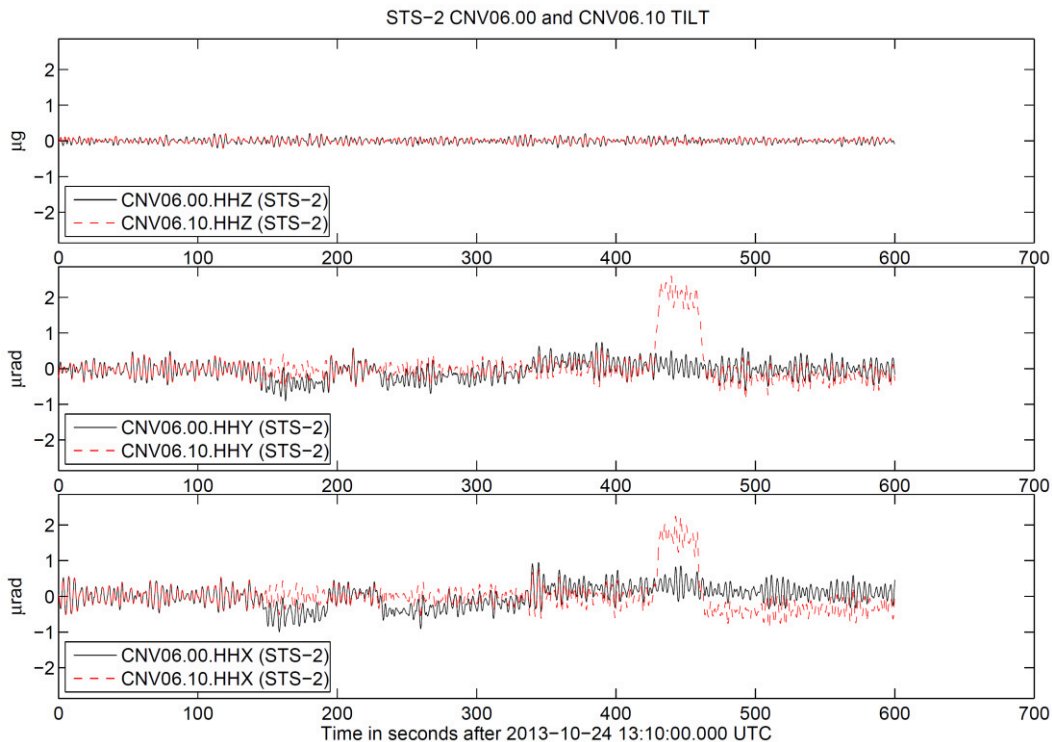
Figure 16: The tilt of the ground at points CNV06.00 (black) and CNV06.10 (red) during the on-site inspection derived by a careful processing of the ground motion velocity time series shown in Figure 14 (details see text). The tilt of the ground during the period with two persons standing in experimental hutch 2 about 0.5 m next to CNV06.10 (seconds 420-480) exceed 2 µrad.

19

The tilt at CNV08.00 due to the two persons standing in the corridor reaches about 5 µrad. The apparent tilt in the later part (after second 350 in Figure 15) is a processing artefact. The x-y-plot in Figure 17 (left) shows the tilt vector pointing towards the surface load in the corridor (compare with x-y coordinates in Figure 1).

The tilt at CNV06.10 due to the two persons standing in experimental hutch 2 reaches about 3 µrad. Again the direction of the tilt vector shown in Figure 17 (right) points towards the location of the two persons in respect to CNV06.10 in the x-y-coordinate system.
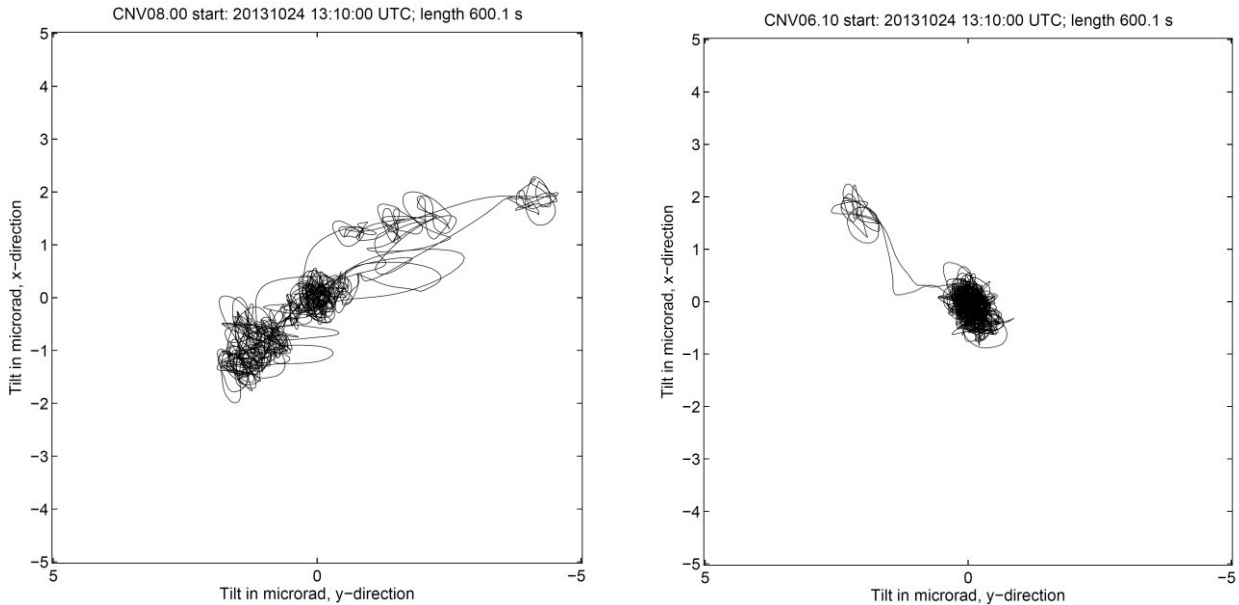
Figure 17: X-Y-Plots of the tilt vectors pointing towards the surface loads during the on-site inspection at point CNV08.00 (left, two persons standing in the corridor eastwards of the IMAGE hutch) and CNV06.10 (right, two persons standing in the hutch about 0.5 apart). See red crosses in Figure 1 (top right).

6.1.1 Tilt of the ground by tram passages

A further source of ground tilt is the passage of tram trains directly north of the ANKA facility (shortest distance to IMAGE experimental hutch 2 about 35 m). The arrival and departure of a tram train is clearly visible in the ground motion velocity time series at points CNV06.00 (black) and CNV08.00 (red) shown in Figure 18. Signals caused by the train are observed at high frequencies (5-30 Hz) on the vertical component as well as low frequencies (below 0.1 Hz) at the horizontal components. The seismic signals on the vertical component have to be interpreted as surface waves caused by the interaction between the tram and the rails and vibrations of the train itself.

The low frequency signals indicate the tilt of the ground due to the passage of the heavy train. The corresponding time series of the ground tilt are shown in Figure 19. The tilt reaches about 0.1 µrad during the departure of the train. The larger tilt during departure may be caused by a larger mass of the train due to in total more passengers leaving KIT at closing time or by the slower speed of the train during departure. The recorded passage lasts about 30 seconds during arrival and about 70 seconds during departure. Due to the short distance between the train station and ANKA it can be assumed that the trains are still accelerating to schedule speed when passing ANKA during departure. The larger tilt at

point CNV08.00 at the rim of the older original ANKA foundation in comparison to point CNV06.00 in the IMAGE experimental hutch 2 less than 2 m apart but on the new foundation indicates a different reaction of the two separated foundations to the passage of the train. This might lead to a relative movement of the entire IMAGE experiment in respect to the beam when a train passes ANKA.
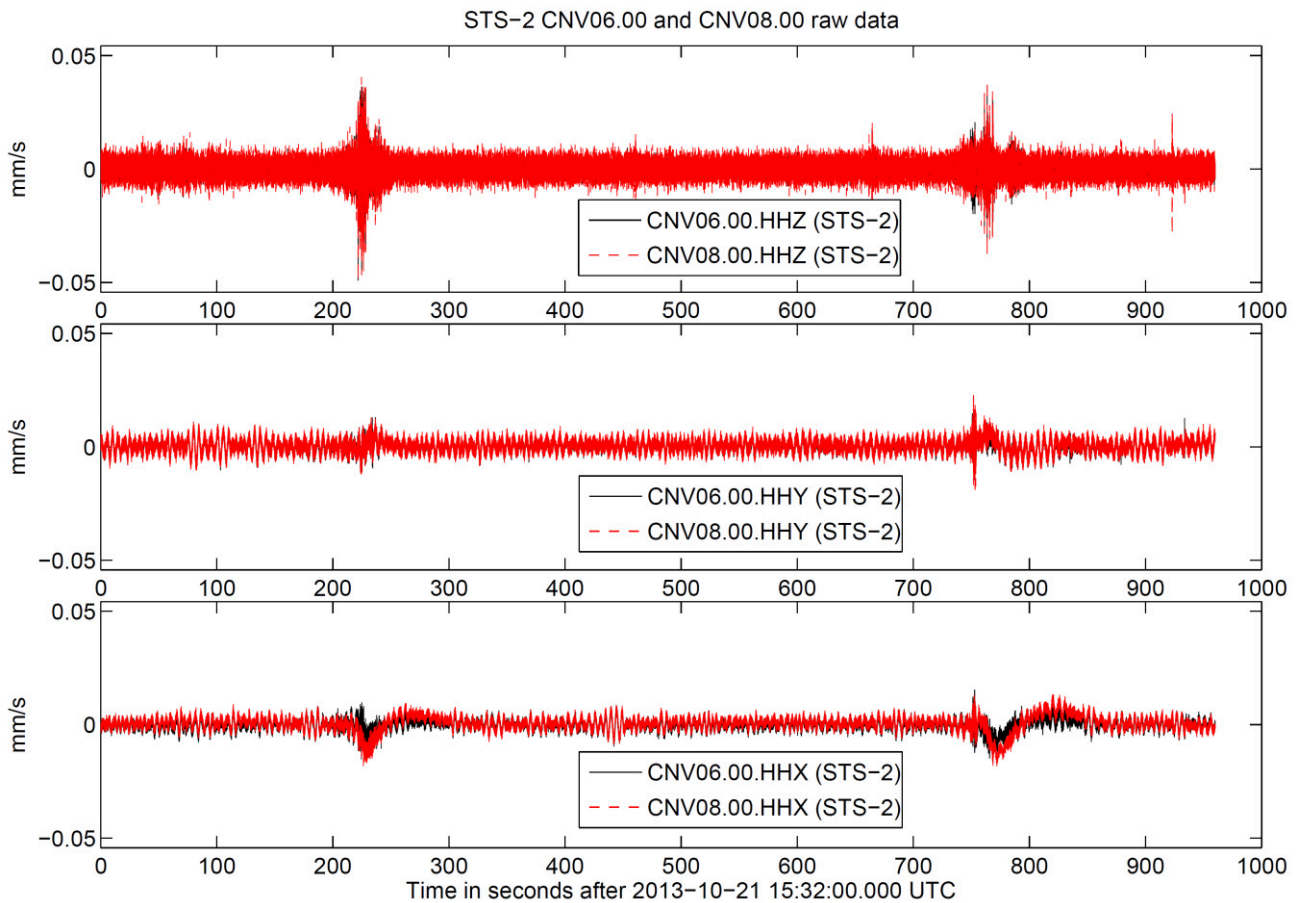
Figure 18: Apparent ground motion velocity observed by the broadband STS-2 seismometers at measurement points CNV06.00 (black) and CNV08.0 (red) during the arrival (seconds 200-250) and departure (seconds 720-900) of a tram train at KIT CN. The high frequency signals observed at the vertical component are travelling seismic waves caused by the interaction of the train with the trails. The long period signals on the horizontal components indicate the tilt of the ground due to the passage of the heavy train.

In Figure 20 the tilt vectors at the points CNV06.00 during the arrival (left) and departure (right) are plotted with color indicating time (cold colors indicate earlier times, hot colors indicate later times). The arrival and departure of the train is reflected by the different sense of the tilt vectors which point towards the shortest distance to the rails.
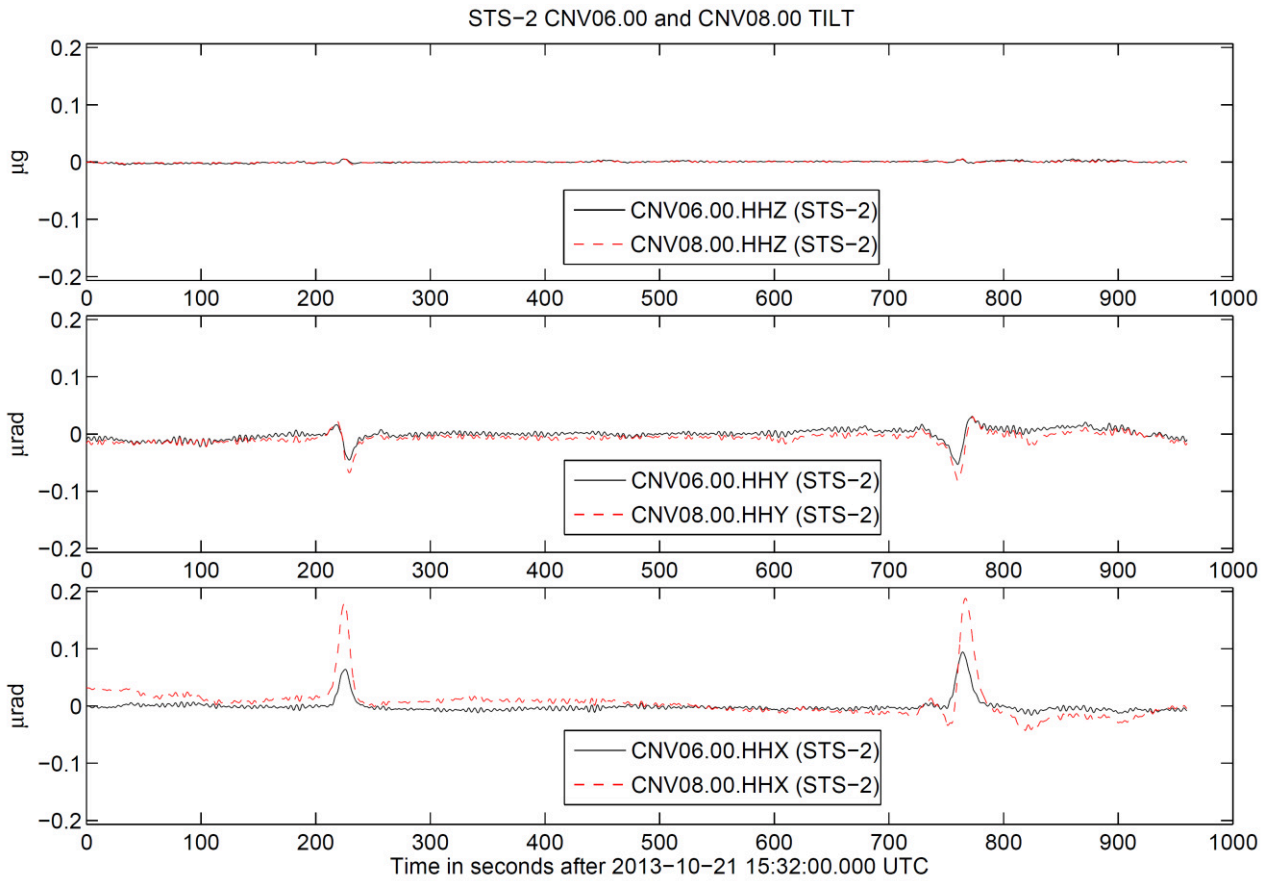
Figure 19: Ground tilt at points CNV06.00 (black) and CNV08.00 (red) derived from the ground motion velocity measurements shown in Figure 18. The passage of the train takes longer during departure (about 70 s) than during arrival (about 30 s). The ground tilt is larger at point CNV08.00 indicating a different reaction of the separated foundations to the passage of the train.
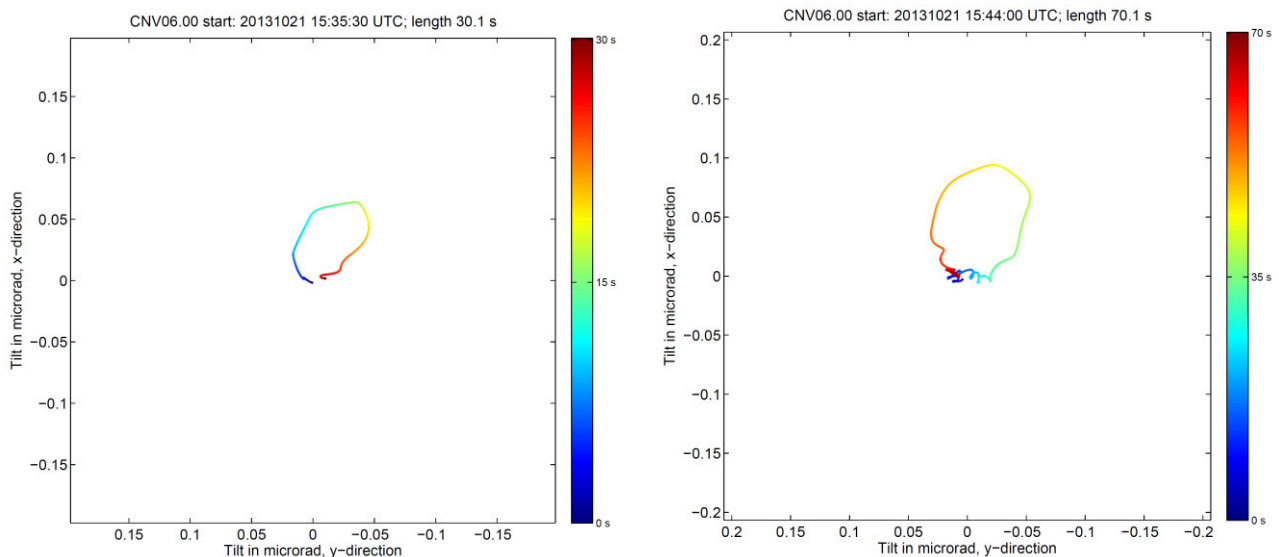
Figure 20: X-Y-Plots of the tilt vectors at point CNV06.00 pointing towards the shortest distance to the tram rails during arrival of the train (left) and departure of the train (right). The color indicates time during passage (cold colors are earlier times). The sense of the tilt vectors matches the direction of the train passages.

22

7 Summary

The Geophysical Institute of the KIT conducted measurements of the ground motion velocity with sensitive broadband seismometers at six measurement points within the IMAGE beamline experimental hutch 2 at ANKA. Purpose of the measurement is the quantitative assessment of the ground motions for the design of a work-place table with active and passive vibration insulation. The measurements provide a data set with undisturbed ground motion time series in the frequency range 0.008 Hz to 90 Hz in the time period 17-Oct-2013 00:00 local time until 30-Oct-2013 23:00 local time (14 days, calendar weeks 42-44).

The ground motion velocities are analyzed in the time and frequency domain in two major frequency ranges: 1-90 Hz (dominating man-made vibrations) and 0.008-1 Hz (natural vibrations and ground tilt due to moving masses).

Above 1 Hz the vertical ground motion velocities are about 2.5 times larger than on the horizontal components. The largest ground motion velocities are observed due to man-made transient signals during daytime at working days in the frequency range 1-30 Hz with exceptional Peak Ground Velocities (PGV) up to 0.2 mm/s. More than 99% of the observed seismic signals exhibit PGV values smaller than 0.1 mm/s (at night time below 0.03 mm/s). The ground motion velocities are significantly decreasing towards frequencies above 30 Hz. Between 10 Hz and 90 Hz several prominent periodic vibrations most probably caused by electrically driven machinery are observed. The most prominent signal at 16.7 Hz exhibits PGV values of about 1 µm/s and average RMS amplitudes of about 0.5 µm/s. This periodic signal shows furthermore a perfect temporal correlation with the beam operation at ANKA. The periodic signal excited by the helium compressor of the Institute of Technical Physics (10 Hz, RMS 5-10 µm/s) known from previous seismic measurements at KIT CN was not observed during the measurement period.

Below 1 Hz the natural sources such as ocean-generated microseism and earthquakes dominate the observed ground motions. The horizontal ground motions are at least 1.5 times larger than the vertical ground motions. An influence of man-made seismic signals on the ground motions is observed down to 0.6 Hz. The largest ground motions in the measurement period are observed due to the body and surface waves of an earthquake off the East coast of Honshu, Japan (magnitude 7.1, distance ~10.000 km). These transient signals reach PGV values between 0.05 mm/s to 0.08 mm/s. Signals due to global seismicity may easily reach PGV values of about 0.5 mm/s and larger at ANKA depending on magnitude and distance. Below 0.1 Hz apparent long period transient signals are observed on the horizontal components which are caused by temporary local ground tilt due to moving masses. Persons entering the hutch or walking outside the hutch close to the hutch walls (especially in the narrow corridor east of experimental hutch 2) cause an observable tilt of the ground up to several µrad in distances up to 1-2 m. Passages of tram trains at the rails about 35 m NNE of the IMAGE experimental hutch 2 are observed to cause a temporary tilt of the ground of about 0.2 µrad. Due to the significant decrease of the ground tilt with distance it has to be expected that passing trains cause a relative movement between the entire IMAGE experiment and the beam provided by ANKA.

8 References

Acernese, F. and the VIRGO working group, 2007. Analysis of noise lines in the Virgo C7 data. *Classical and Quantum Gravity*, **24**, 433-443.

Bonnefoy-Claudet, S., Cotton, F. & Bard, P.-Y., 2006. The nature of noise wavefield and its applications for site effects studies: A literature review. *Earth-Sci. Rev.,* **79,** 205–227.

Coward, D., Blair, D., Burman, R. & Zhao, C., 2003. Vehicle-induced seismic effects at a gravitational wave observatory. *Review of Scientific Instruments,* **74,** 4846–4854.

Coward, D., Turner, J., Blair, D. & Galybin, K., 2005. Characterizing seismic noise in the 2-20 Hz band at a gravitational wave observatory. *Review of Scientific Instruments,* **76,** 44501-1–44501-5.

Groos, J. C. & Ritter, J. R. R., 2009. Time domain classification and quantification of seismic noise in an urban environment. *Geophysical Journal International,* **179,** 1213–1231.

Groos, J. C., 2010. Broadband seismic noise: Classification and Green's Function Estimation, *Dissertation*, Karlsruhe Institute of Technology, Germany, 155pp.

Groos, J. & Ritter, J. R. R., 2010. Seismic noise: A challenge and opportunity for seismological monitoring in densely populated areas in Ritter, J. & Oth, A. (Eds.), Induced Seismicity, Cahiers du Centre Européen de Géodynamique et de Séismologie, **30**, 87-97, 2010.

Groos J. & Ritter, J. R. R., 2011. Bericht zu den seismischen Messungen an den Standorten KATRIN und ANKA auf dem KIT Campus Nord im November und Dezember 2011, *KIT Internal Report*, Karlsruhe Institute of Technology, Germany, 35pp.

Ritter, J. R. R. & H. Sudhaus, 2007. Characterization of small local noise sources with array seismology, *Near Surface Geophysics*, **5**, 253-261.

Wielandt, E. & T. Forbriger, 1999. Near-field seismic displacement and tilt associated with the explosive activity of Stromboli, *Annali Di Geofisica*, **42**, 407-416.

Wielandt, E., 2011. Chapter 5: Seismic Sensors and their Calibration in Bormann, P. (Ed.), New Manual of Seismological Observatory Practice (NMSOP-2), IASPEI, GFZ German Research Centre for Geosciences, Potsdam; http://nmsop.gfz-potsdam.de, DOI: 10.2312/GFZ.NMSOP-2, 2012.

9 Appendix
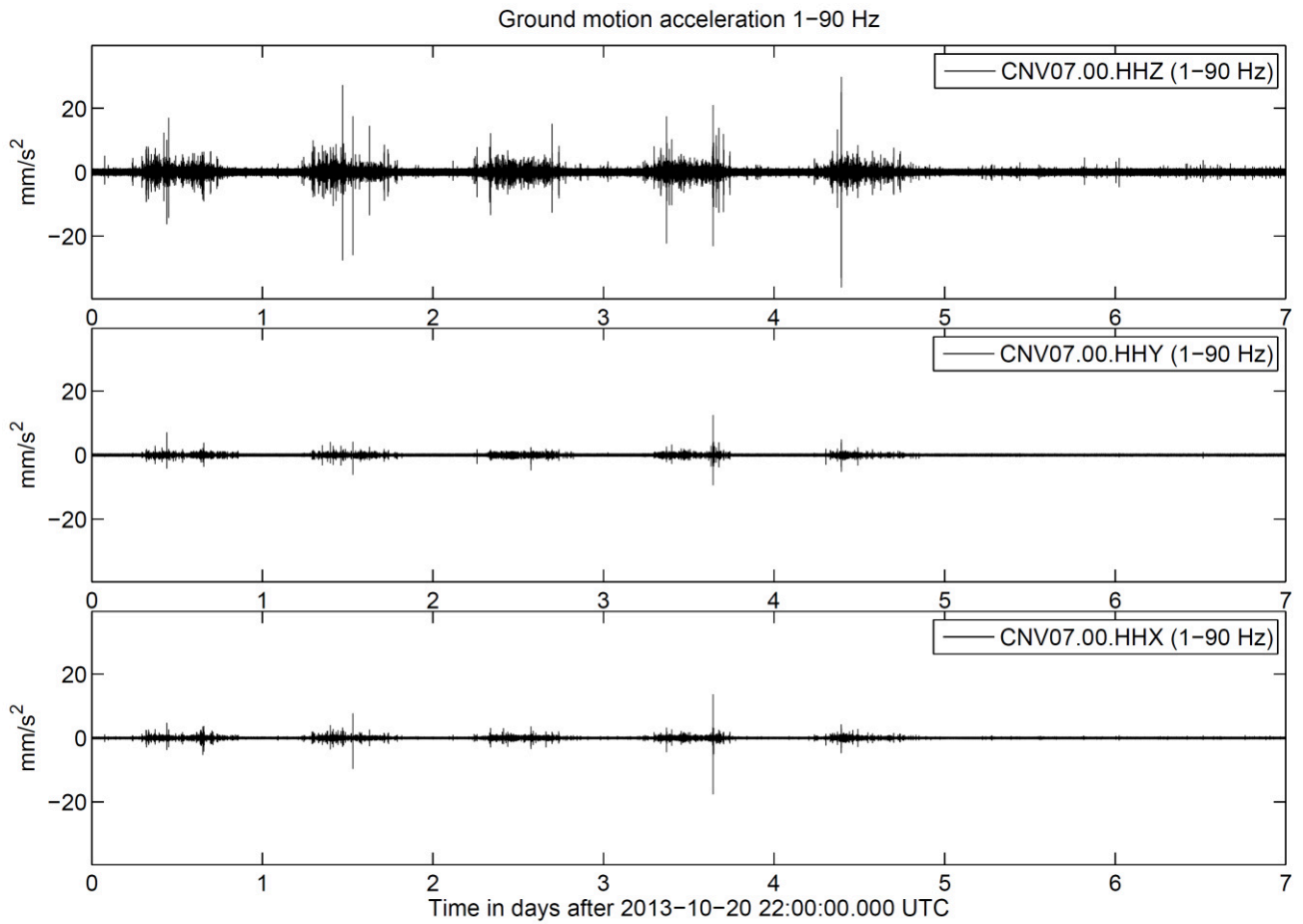
Figure 21: Ground motion acceleration on the vertical (Z, top) and the two horizontal (Y, middle and X, bottom) components in the frequency range 1-90 Hz at measuring point CNV07.00 during calendar week 43. The horizontal component coordinates correspond to the beamline coordinates (see Figure 1).
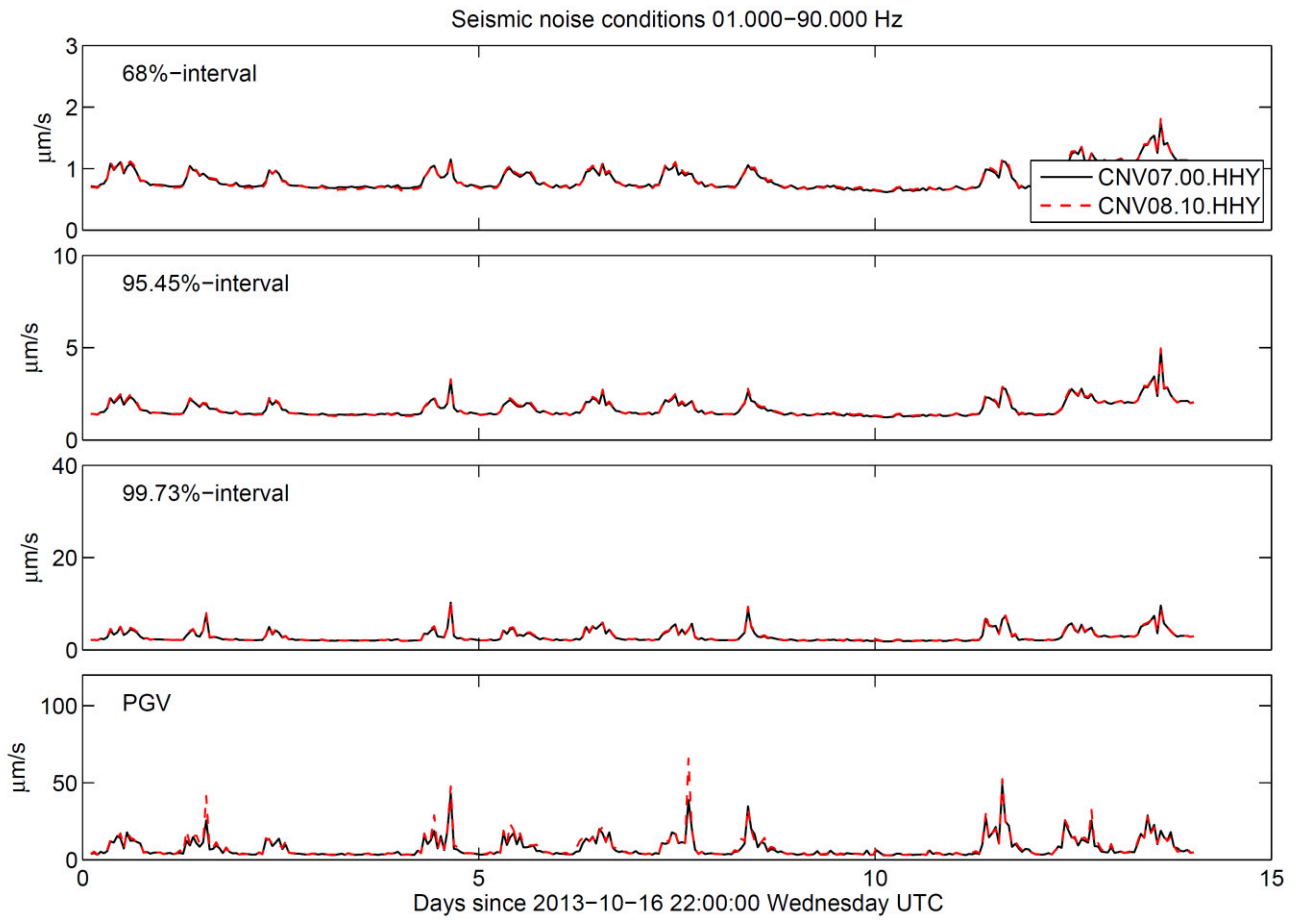
Figure 22: Statistical quantification of the horizontal (Y-component) ground motion velocities in the frequency range 1-90 Hz at measurement points CNV07.00 (red) and CNV08.10 (black). Shown are the upper boundaries of the (from top to bottom) 68%, 95.45%, 99.73% and 100% (PGV) amplitude intervals described in Figure 2. The quantities are determined with a sliding time window (window and step length 1 hour) for the time period 17-Oct-2013 to 30-Oct-2013.
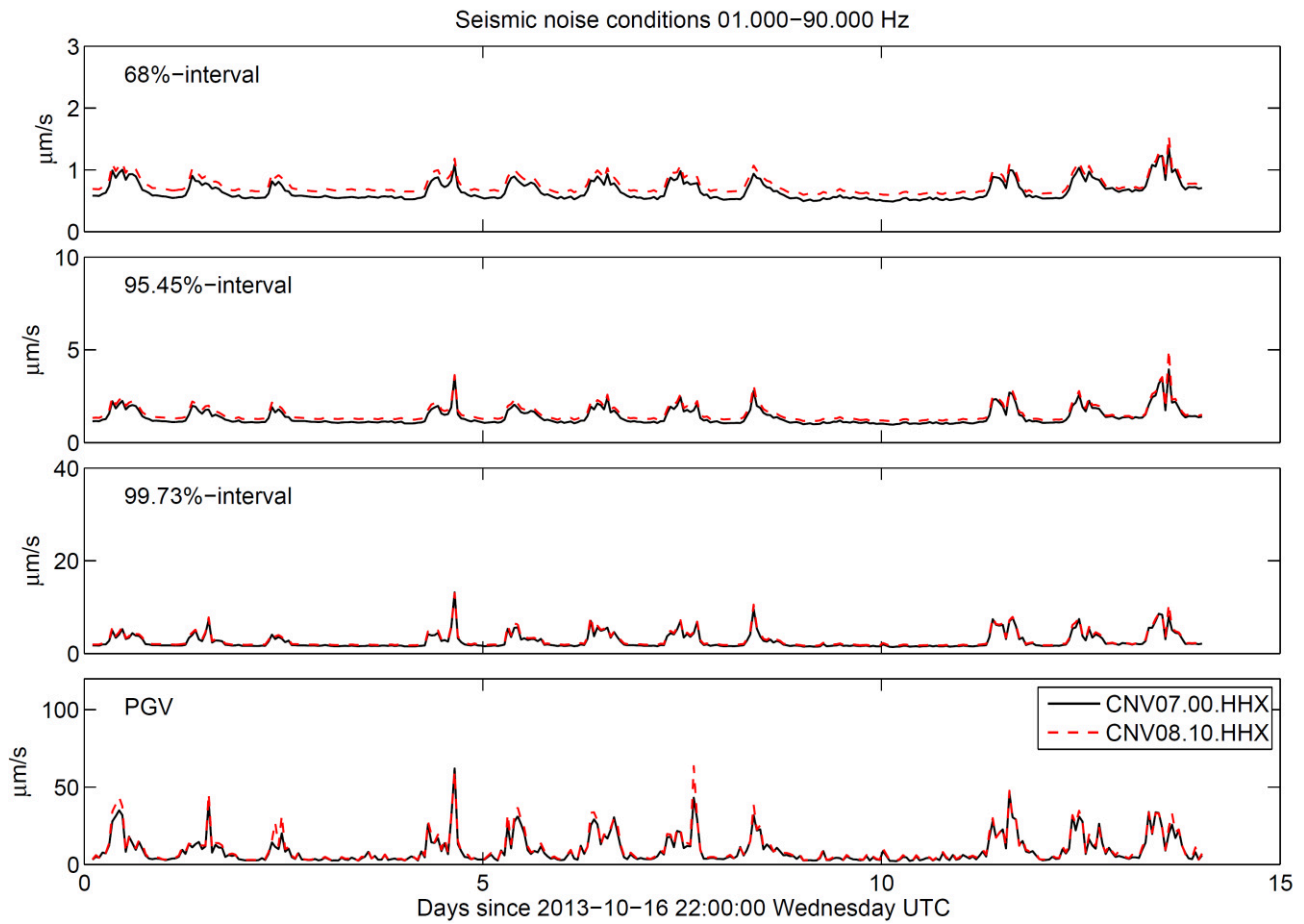
Figure 23: Statistical quantification of the horizontal (X-component) ground motion velocities in the frequency range 1-90 Hz at measurement points CNV07.00 (red) and CNV08.10 (black). Shown are the upper boundaries of the (from top to bottom) 68%, 95.45%, 99.73% and 100% (PGV) amplitude intervals described in Figure 2. The quantities are determined with a sliding time window (window and step length 1 hour) for the time period 17-Oct-2013 to 30-Oct-2013.